Full QED calculations of two-photon exchange for heliumlike-systems: Analysis in the Coulomb and Feynman gauges

Ingvar Lindgren, Hans Persson, and Sten Salomonson
Department of Physics, Chalmers University of Technology and the University of Gothenburg, S-412 96 Göteborg, Sweden

Leonti Labzowsky
St. Petersburg State University, 198904 Petrodvorets, St. Petersburg, Russia
(Received 30 June 1994)

A complete, numerical calculation of the effect of the exchange of two virtual photons between the electrons in the ground states of heliumlike systems is presented. Feynman diagrams with uncrossed and crossed photons are evaluated, using the Furry interaction picture [Phys. Rev. **81**, 115 (1951)], neglecting nuclear recoil. The calculations are carried out in the Feynman gauge as well as in the Coulomb gauge, and the gauge invariance of this set of diagrams is verified with high numerical accuracy. The numerical technique employed is similar to that recently developed for our self-energy calculations [H. Persson, I. Lindgren, and S. Salomonson, Phys. Scrip. **T46**, 125 (1993); I. Lindgren, H. Persson, S. Salomonson, and A. Ynnerman, Phys. Rev. A **47**, R4555 (1993)]. An explicit summation is performed over a complete set of intermediate states with positive and negative energy, generated with the technique of discretization. The photon propagators are expanded in spherical waves, and the radial integrations are performed numerically using analytical Bessel functions. Also the integration over the photon energy is performed numerically. The calculations are performed for different values of the nuclear charge in the range $Z = 2$–92. Corresponding calculations are also performed without retardation and neglecting the effect of negative-energy states (virtual electron-positron pairs), thus simulating relativistic many-body calculations in the no-virtual-pair approximation. The difference, which in this way is obtained with high numerical accuracy, represents the "quantum electrodynamics (QED) correction," which should be added to the many-body result in a combined QED-many-body procedure. The various contributions to the two-photon exchange have been analyzed in detail and compared with the analytical results to order $(Z\alpha)^3$ of Sucher [Phys. Rev. **109**, 1010 (1958)]. From our analysis, general conclusions can also be drawn concerning the accuracy of various relativistic many-body approaches.

PACS number(s): 31.10.+z, 31.20.Di, 31.30.Jv

I. INTRODUCTION

The interest in the application of relativistic many-body perturbation theory (RMBPT) to atomic systems has increased significantly in recent years, mainly due to the development in heavy-ion spectroscopy. It is now possible to study virtually any ion of the Periodic Table up to hydrogenlike uranium [1]. Most RMBPT calculations are based on the so-called *no-virtual-pair approximation*, where the effect of negative-energy states (virtual electron-positron pairs) as well as radiative effects are omitted [2–4]. Using the Coulomb gauge, this approximation is for low Z correct to the order $(Z\alpha)^2$ hartree atomic units (hartree) or $\alpha^2(\alpha Z)^2$ in relativistic units. This accuracy is usually sufficient for applications on low-Z systems or when studying the outer electrons of heavier systems (for which the "effective" nuclear charge is still rather small). On the other hand, for heavy, highly charged ions, or in studying *inner* holes on any heavy system, effects beyond the no-virtual-pair approximation become quite significant.

The single-electron Lamb shift is of the order $Z(Z\alpha)^3$ hartree for low Z and becomes comparable to the electron correlation already in the first half of the Periodic Table. The virtual pairs have leading contributions of the orders $(Z\alpha)^3\ln(Z\alpha)$ and $(Z\alpha)^3$ and become comparable to the electron correlation for high Z. Other effects that enter in the order $(Z\alpha)^3$ are the retardation effect and the many-electron correction to the Lamb shift ("screening"). Also the second-order Breit interaction (Breit-Breit) is of this order [5–9].

We have recently developed a new technique of evaluating the Lamb shift for heavy ions, applied to lithium-like uranium [10], where new experimental information has recently become available [11]. This technique is based on the generation of a complete set of solutions of the single-electron Dirac equation, using the method of discretization, developed by Salomonson and Öster [12]. The technique is also well adapted for the evaluation of other kinds of QED effects and we present here a complete evaluation of the two-photon exchange between the electrons of He-like systems. Similar calculations have recently been performed also by Blundell *et al.* [9], using a different evaluation procedure and, where a comparison can be made, the numerical agreement between the two calculations is found to be very good. We are presently

also involved in the evaluation of other two-photon effects in few-electron systems, such as the combined self-energy vacuum-polarization and combined self-energy–self-energy effects, which are reported elsewhere [13–15].

The work presented here represents a step toward the construction of a *combined many-body–QED procedure* [16,17]. For very highly charged, heavy ions, single-electron radiative effects dominate over the many-body (correlation) effects and it is then a good procedure to base the treatment entirely on the QED formalism, i.e., treating successively one-, two-, etc., photon effects in a rigorous manner. For less highly charged systems, on the other hand, the many-body effects become more important and they are usually slowly converging. It would then be a hopeless task to perform an accurate calculation for such a system by evaluating all relevant diagrams in a complete Feynman manner. We know, however, that for such systems the many-body perturbation theory approach or the coupled-cluster approach yields quite accurate results [18–24]. Here the most important many-body effects (in the no-virtual-pair approximation) are included to high (essentially all) orders. It would then be much more economical to use such a calculation as the starting point and to add the remaining effects by means of successive approximations. This can be done in a rigorous way by means of effective potentials, based on one-, two-, etc., photon interactions between the electrons [16,25].

Treating the nucleus as fixed, i.e., neglecting nuclear recoil, we can define a Hamiltonian for an N-electron system in the following way:

$$H = \sum_{n=1}^{N} h_D(n) + \sum_{m<n}^{N} V_{mn} + \sum_{m<n<p}^{N} V_{mnp} + \cdots \ . \quad (1.1)$$

Here h_D is the single-electron Dirac Hamiltonian and V_{mn}, V_{mnp}, ... are effective two-, three-, etc., electron potentials, defined by means of QED. The effect of the three-electron potential (and beyond) can be expected to be very small [26] and we shall restrict ourselves here to the effective two-electron potential V_{mn}. This can be separated into one-, two-, etc., photon contributions

$$V_{mn} = V_{mn}^{(1)} + V_{mn}^{(2)} + V_{mn}^{(3)} + \cdots \ . \quad (1.2)$$

The one-photon potential $V_{mn}^{(1)}$ is the interaction used in the many-body calculation and the two-photon potential $V_{mn}^{(2)}$ represents the remaining (irreducible) part of the two-photon exchange, which is not taken care of by iterating the one-photon potential, i.e., performing a many-body calculation. In a similar way $V_{mn}^{(3)}$ can be defined as the irreducible part of the three-photon interaction, which is not taken care of by iterating $V_{mn}^{(1)}$ and $V_{mn}^{(2)}$, etc. The analysis of the present work yields only a part of the two-photon potential, which gives the lowest-order QED energy correction to the RMBPT ground-state energy. Similar calculations will be performed for excited states of heliumlike ions. In principle, it will be possible to calculate the three-photon potential in a similar way, although its effect on the level structure will be quite small. Radiative effects (electron self-energy, vacuum polarization, etc.) can be treated separately and are not considered in the present work.

It is well known that the results of QED are gauge independent in each order of the perturbation theory. This is true also for certain subgroups of contributions in each order. For instance, for two-electron systems the self-energy contributions, where the photons interact with only one electron, are gauge independent separately from the contributions involving two electrons. Nevertheless, a significant gauge dependence has been observed when the electron correlation for heliumlike systems is evaluated by means of many-body techniques using different effective single-photon potentials derived from QED. In particular, it was shown that potentials obtained in the Feynman and the Coulomb gauges lead to different numerical results in self-consistent-field (SCF) calculations of Dirac-Fock type for such systems [27]. The reason for this was found to be due to the fact that SCF methods, as well as any other method based on the iterative use of single-photon potentials, yield only a part of the higher-order QED diagrams. In the second-order the crossed-photon diagram [Fig. 1(b)] and a part of the uncrossed-photon diagram [Fig. 1(a)] are omitted. It has been shown that these effects are significantly larger in the Feynman gauge than in the Coulomb gauge and this caused the observed discrepancy [28,29].

It can be argued that the combined many-body–QED procedure, suggested here, is *not* gauge invariant since the many-body effects are evaluated to high orders and the QED effects only to low orders. This is certainly the case, but this is not expected to cause any major difficulty in actual applications. In principle, it is possible to apply the procedure from a one-photon potential, derived in any gauge, as long as the remaining parts are correctly taken care of by the many-photon potentials. The main point is that the many-body and the QED calculations should be exactly *compatible*. The size of the QED corrections, though, can be considerably different in different gauges, as will be demonstrated in the present work. This size can be used as an indication of the accuracy of the procedure. For low- and medium-heavy elements the one-photon potential from the Coulomb gauge is known to be a considerably better approximation than that of the Feynman gauge and can therefore be expected to lead to faster convergence.

In this work we have investigated the two-photon exchange between the electrons of heliumlike systems, using the Coulomb gauge, for the nuclear charge in the range $Z = 2 - 92$. For $Z = 2, 10$, and 80 the calculations are performed also in the Feynman gauge and the gauge independence between the two gauges is demonstrated with very high numerical accuracy. The importance of the crossed-photon diagram, particularly in the Feynman gauge, is verified. For $Z = 10$ this contribution is of the order of 10% of the leading second-order Coulomb-Coulomb correlation. The calculations are also performed *without retardation* and neglecting virtual pairs, thus simulating a second-order RMBPT calculation in the no-virtual-pair approximation without retardation. By doing the retarded and unretarded cal-

culations with the same numerical procedure, same grid points, etc., the difference is obtained with much higher numerical accuracy than by taking the difference between two independent calculations, using different techniques. This difference represents the lowest-order QED correction to be used in the combined many-body–QED procedure, indicated above. The various contributions to this correction, such as the effect of retardation and single and double virtual pairs, are analyzed in terms of an αZ expansion in order to compare with the available analytical results of Sucher [6] and Araki [30].

The paper is organized as follows. In the next section we derive the formulas needed for the evaluation of the uncrossed- and crossed-photon diagrams in the two gauges. In Sec. III we present the numerical procedure and the numerical results. The QED corrections to the many-body results, evaluated in the way indicated above, are analyzed in Sec. IV. Some general conclusions, which can be drawn from the present analysis, concerning the accuracy of different RMBPT approaches, are presented in Sec. V.

II. EVALUATION OF THE TWO-PHOTON DIAGRAMS

The exchange of two virtual photons between two electrons is represented by the two Feynman diagrams in Fig. 1, the first (a) with uncrossed photons ("ladder" or "box" diagram) and the second (b) with crossed photons ("crossed ladder"). The energy shift due to these effects are given by the formula derived in 1957 by Sucher [6]

$$\Delta E_A = \lim_{\gamma\to 0}\frac{1}{2}i\gamma\{4\langle\Phi_a^0 \mid S^4_{\mathrm{lad},\gamma}\mid\Phi_a^0\rangle + 4\langle\Phi_a^0 \mid S^4_{\mathrm{cro},\gamma}\mid\Phi_a^0\rangle - 2\langle\Phi_a^0 \mid S^2_{\gamma}\mid\Phi_a^0\rangle^2\}. \quad (2.1)$$

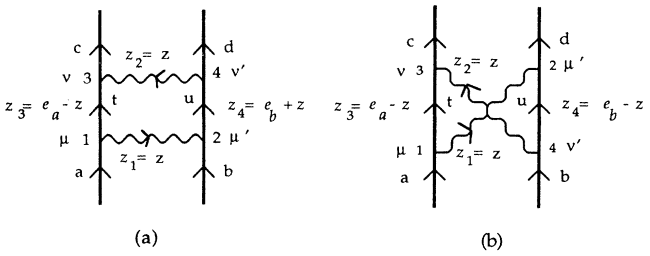

FIG. 1. Feynman diagrams representing the two-photon exchange between two electrons with (a) uncrossed and (b) crossed photons.

In the case of the ground state of He-like atoms, we can restrict ourselves to equivalent electrons in the initial and final states (same n, l, and j).

For the ladder contribution, intermediate states which are degenerate with the initial (reference) state lead to a singularity which is canceled by the squared second-order S-matrix contribution. After removing the singularity, such states also give rise to a finite contribution [31,8,9]. The degenerate states, both for the uncrossed and crossed diagram, and the squared second-order contribution are left out of the discussion in this section and are treated separately in Appendix A.

A. Feynman gauge: Uncrossed photons

We consider first the uncrossed diagram in Fig. 1(a). The S-matrix element for this diagram is ($\hbar$=1)

$$\langle\Phi_a^0 \mid S^4_{\mathrm{lad},\gamma}\mid\Phi_a^0\rangle = (ie)^4\int d^4x_1\int d^4x_2\int d^4x_3\int d^4x_4 e^{-\gamma|t_3|}e^{-\gamma|t_1|}\Phi_c^\dagger(x_3)\alpha_3^\nu iS_F(x_3,x_1)\alpha_1^\mu\Phi_a(x_1)$$
$$\times e^{-\gamma|t_4|}e^{-\gamma|t_2|}\Phi_d^\dagger(x_4)\alpha_4^{\nu'}iS_F(x_4,x_2)\alpha_2^{\mu'}\Phi_b(x_2)\frac{i}{c}D_{F\nu\nu'}(x_3-x_4)\frac{i}{c}D_{F\mu'\mu}(x_2-x_1), \quad (2.2)$$

where the photon propagator in the Feynman gauge is defined by

$$D_{F\nu\mu}(x_2-x_1) = -\frac{1}{\epsilon_0}g_{\nu\mu}\int\frac{d^4k}{(2\pi)^4}\frac{e^{-ik(x_2-x_1)}}{(k^2+i\epsilon)} = \int\frac{dz}{2\pi}e^{-iz(t_2-t_1)}D_{F\nu\mu}(\mathbf{x}_2-\mathbf{x}_1,z) \quad (2.3)$$

and

$$D_{F\nu\mu}(\mathbf{x}_2-\mathbf{x}_1,z) = -\frac{c}{\epsilon_0}g_{\nu\mu}\int\frac{d^3\mathbf{k}}{(2\pi)^3}\frac{e^{i\mathbf{k}\cdot(\mathbf{x}_2-\mathbf{x}_1)}}{(z^2-c^2\mathbf{k}^2+i\epsilon)}. \quad (2.4)$$

We have defined here the z parameter by $k=(z/c,\mathbf{k})$. The electron propagator is defined by

$$S_F(x_2,x_1) = \sum_s\int\frac{dz}{2\pi}e^{-iz(t_2-t_1)}\frac{\Phi_s(\mathbf{x}_2)\Phi_s^\dagger(\mathbf{x}_1)}{z-e_s(1-i\eta)} = \int\frac{dz}{2\pi}e^{-iz(t_2-t_1)}S_F(\mathbf{x}_2,\mathbf{x}_1,z), \quad (2.5)$$

where η is a small positive number. The time-dependent eigenfunction is given by

$$\Phi_s(x) = e^{-ie_st}\Phi_s(\mathbf{x}). \quad (2.6)$$

We use here the Furry interaction picture [32] with the single-electron states $\Phi_s(\mathbf{x})$ being solutions of the time-independent Dirac equation with a Coulomb nuclear potential V,

$$h_D\Phi_s(\mathbf{x}) = e_s\Phi_s(\mathbf{x}), \quad (2.7)$$

where

$$h_D = c\boldsymbol{\alpha}\cdot\mathbf{p} + \beta mc^2 + V. \tag{2.8}$$

(This implies that nuclear recoil is neglected.) The time integrations in Eq. (2.2) are trivial to perform, leading to energy conservation at the vertices (in the limit where the adiabatic damping factor $\gamma \to 0$). The remainder of Eq. (2.2) reduces to a space integral M (the Feynman amplitude)

$$\begin{aligned} M = & \int d^3x_1 \int d^3x_2 \int d^3x_3 \int d^3x_4 \int \frac{dz}{2\pi} \\ & \times \Phi_c^\dagger(\mathbf{x}_3) iec\alpha_3^\nu i S_F(\mathbf{x}_3,\mathbf{x}_1,e_a - z) iec\alpha_1^\mu \Phi_a(\mathbf{x}_1) \\ & \times \Phi_d^\dagger(\mathbf{x}_4) iec\alpha_4^{\nu'} i S_F(\mathbf{x}_4,\mathbf{x}_2,e_b + z) iec\alpha_2^{\mu'} \Phi_b(\mathbf{x}_2) \\ & \times \frac{i}{c} D_{F\nu\nu'}(\mathbf{x}_3 - \mathbf{x}_4, z) \frac{i}{c} D_{F\mu'\mu}(\mathbf{x}_2 - \mathbf{x}_1, z) \end{aligned} \tag{2.9}$$

or alternatively, by using the explicit representation of the photon and electron propagators, we obtain

$$\begin{aligned} M = & \left(\frac{e^2c^2}{\epsilon_0}\right)^2 \sum_{t,u} \int \frac{dz}{2\pi} \left\langle cd \left| \alpha_4^\nu \alpha_{\nu 3} \int \frac{d^3\mathbf{k}'}{(2\pi)^3} \frac{e^{i\mathbf{k}'\cdot(\mathbf{x}_3-\mathbf{x}_4)}}{(z^2 - \mathbf{k}'^2 + i\epsilon)} \right| tu \right\rangle \left\langle tu \left| \alpha_2^\mu \alpha_{\mu 1} \int \frac{d^3\mathbf{k}}{(2\pi)^3} \frac{e^{i\mathbf{k}\cdot(\mathbf{x}_2-\mathbf{x}_1)}}{(z^2 - \mathbf{k}^2 + i\epsilon)} \right| ab \right\rangle \\ & \times \frac{1}{[e_a - z - e_t(1 - i\eta)]} \frac{1}{[e_b + z - e_u(1 - i\eta')]}. \end{aligned} \tag{2.10}$$

The standard procedure in evaluating expressions of this type is first to perform the Fourier integration in the matrix elements, which yields the effective electron-electron interaction in the Feynman gauge

$$\begin{aligned} V_{12}(z) &= \alpha_1^\mu \alpha_{\mu 2} \frac{e^2c^2}{\epsilon_0} \int \frac{d^3\mathbf{k}}{(2\pi)^3} \frac{e^{i\mathbf{k}\cdot(\mathbf{x}_2-\mathbf{x}_1)}}{(z^2 - c^2\mathbf{k}^2 + i\epsilon)} \\ &= \alpha_2^\mu \alpha_{\mu 1} \frac{e^2c^2}{\epsilon_0} \frac{e^{i\sqrt{z^2 + i\eta r_{12}}}}{r_{12}}, \end{aligned} \tag{2.11}$$

where the square root with a positive imaginary part is chosen. Then the z integration is performed using a Wick rotation in the complex plane. Here we shall instead follow the procedure we developed in our self-energy calculations [10] and start with the z integration.

We begin by evaluating the integral

$$\begin{aligned} I = & \int_{-\infty}^{\infty} \frac{dz}{2\pi} \frac{1}{(q - z + i\eta_t)} \frac{1}{(q' + z + i\eta_u)} \\ & \times \frac{1}{[z^2 - (ck' - i\eta)^2]} \frac{1}{[z^2 - (ck - i\eta)^2]}, \end{aligned} \tag{2.12}$$

where $q = e_a - e_t$ and $q' = e_b - e_u$ and η_t and η_u have the same sign as e_t and e_u, respectively. (We have used here the fact that $k = |\mathbf{k}|$ is positive.) For particular *positive* values of the intermediate energies e_t and e_u, the integral becomes

$$\begin{aligned} I = & \frac{i}{2ckck'(q + q')(ck + ck')} \\ & \times \left\{ \frac{q' - ck - ck'}{(q' - ck)(q' - ck')} + \frac{q - ck - ck'}{(q - ck)(q - ck')} \right\}. \end{aligned} \tag{2.13}$$

Intermediate states degenerate with the reference state are here omitted (see Appendix A). Multiplying the Feynman amplitude by the imaginary unit i yields the corresponding energy contribution

$$\begin{aligned} \Delta E_{\mathrm{lad},tu}^{++} = & -\left(\frac{e^2c^2}{\epsilon_0}\right)^2 \int \frac{d^3\mathbf{k}}{(2\pi)^3} \int \frac{d^3\mathbf{k}'}{(2\pi)^3} \langle ab|\alpha_3^\nu \alpha_{\nu 4} e^{i\mathbf{k}'\cdot(\mathbf{x}_3-\mathbf{x}_4)}|tu\rangle \langle tu|\alpha_1^\mu \alpha_{\mu 2} e^{i\mathbf{k}\cdot(\mathbf{x}_2-\mathbf{x}_1)}|ab\rangle \\ & \times \frac{1}{2ckck'(q + q')(ck + ck')} \left\{ \frac{q' - ck - ck'}{(q' - ck)(q' - ck')} + \frac{q - ck - ck'}{(q - ck)(q - ck')} \right\} \end{aligned} \tag{2.14}$$

where $++$ denotes that t and u are positive energy states. After the integration over the angular parts of k and k' this becomes

$$\begin{aligned} \Delta E_{\mathrm{lad},tu}^{++} = & -\left(\frac{e^2}{2\pi^2\epsilon_0}\right)^2 \int dk \int dk' \left\langle ab \left| \alpha_3^\nu \alpha_{\nu 4} \frac{\sin(k'r_{34})}{k'r_{34}} \right| tu \right\rangle \left\langle tu \left| \alpha_1^\mu \alpha_{\mu 2} \frac{\sin(kr_{12})}{kr_{12}} \right| ab \right\rangle \\ & \times \frac{ckck'}{2(q + q')(ck + ck')} \left\{ \frac{q' - ck - ck'}{(q' - ck)(q' - ck')} + \frac{q - ck - ck'}{(q - ck)(q - ck')} \right\} \end{aligned} \tag{2.15}$$

and by using the spherical-wave expansion

$$\frac{\sin(kr_{12})}{kr_{12}} = \sum_{l=0}^{\infty} (2l + 1) j_l(kr_1) j_l(kr_2) \mathbf{C}^l(1)\cdot\mathbf{C}^l(2) \tag{2.16}$$

we obtain

$$\Delta E^{++}_{\rm lad} = -\left(\frac{e^2}{2\pi^2\epsilon_0}\right)^2 \sum_{l,l'}(2l+1)(2l'+1)\int dk\int dk'\sum_t\sum_u \langle a|\alpha^\nu \mathbf{C}^{l'} j_{l'}(k'r)|t\rangle\cdot\langle b|\alpha_\nu \mathbf{C}^{l'} j_{l'}(k'r)|u\rangle$$
$$\times\langle t|\alpha^\mu \mathbf{C}^{l} j_{l}(kr)|a\rangle\cdot\langle u|\alpha_\mu \mathbf{C}^{l} j_{l}(kr)|b\rangle \frac{ckck'}{2(ck+ck')}\frac{1}{(q+q')}\left\{\frac{q'-ck-ck'}{(q'-ck)(q'-ck')}+\frac{q-ck-ck'}{(q-ck)(q-ck')}\right\}. \quad (2.17)$$

The corresponding expression for general intermediate states will be discussed later.

In the z integration performed here there are contributions from the poles of the electron propagators as well as of the photon propagators. If we consider only the poles of the former, integrating over the upper and lower half planes, we obtain

$$\Delta E^{+}_{\rm el} = \sum_{t,u}\frac{\langle cd|V_{34}(q)|tu\rangle\langle tu|V_{12}(q)|ab\rangle}{q+q'},$$

$$\Delta E^{-}_{\rm el} = \sum_{t,u}\frac{\langle cd|V_{34}(q')|tu\rangle\langle tu|V_{12}(q')|ab\rangle}{q+q'}, \quad (2.18)$$

respectively, where $V_{12}(q)$ is an effective one-photon potential and $q+q' = e_a+e_b-e_t-e_u$. The two contributions are not identical because all poles are not considered. Taking the average of the two contributions yields a more symmetric expression

$$\Delta E^{\pm}_{\rm el} = \frac{1}{2}\sum_{t,u}\left\{\frac{\langle cd|V_{34}(q)|tu\rangle\langle tu|V_{12}(q)|ab\rangle}{q+q'} + \frac{\langle cd|V_{34}(q')|tu\rangle\langle tu|V_{12}(q')|ab\rangle}{q+q'}\right\}. \quad (2.19)$$

This can be approximated by using the potential

$$\langle tu|V_{12}(q,q')|ab\rangle = \frac{1}{2}\{\langle tu|V_{12}(q)|ab\rangle + \langle tu|V_{12}(q')|ab\rangle\} \quad (2.20)$$

in the standard expression of second-order perturbation theory. These relations are valid in any gauge. When the Coulomb gauge is used, the potential in Eq. (2.20) is identical to the *Mittelman potential* [33].

B. Feynman gauge: Crossed photons

The Feynman amplitude for crossed-photon diagram [Fig. 1(b)] can be evaluated in the same way as for uncrossed photons

$$M = \int d^3x_1\int d^3x_2\int d^3x_3\int d^3x_4\int\frac{dz}{2\pi}\Phi^\dagger_c(\mathbf{x}_3)iec\alpha^\nu_3 iS_F(\mathbf{x}_3,\mathbf{x}_1,e_a-z)iec\alpha^\mu_1\Phi_a(\mathbf{x}_1)$$
$$\times\Phi^\dagger_d(\mathbf{x}_2)iec\alpha^{\mu'}_2 iS_F(\mathbf{x}_2,\mathbf{x}_4,e_b-z)iec\alpha^{\nu'}_4\Phi_b(\mathbf{x}_4)\frac{i}{c}D_{F\nu\nu'}(\mathbf{x}_3-\mathbf{x}_4,z)\frac{i}{c}D_{F\mu'\mu}(\mathbf{x}_2-\mathbf{x}_1,z). \quad (2.21)$$

In the Feynman gauge this becomes

$$M = \left(\frac{e^2c^2}{\epsilon_0}\right)^2\sum_{t,u}\int\frac{dz}{2\pi}\left\langle cu\left|\alpha^\nu_3\alpha_{\nu4}\int\frac{d^3\mathbf{k}'}{(2\pi)^3}\frac{e^{i\mathbf{k}'\cdot(\mathbf{x}_3-\mathbf{x}_4)}}{(z^2-c^2\mathbf{k}'^2+i\epsilon)}\right|tb\right\rangle$$
$$\times\left\langle td\left|\alpha^\mu_1\alpha_{\mu2}\int\frac{d^3\mathbf{k}}{(2\pi)^3}\frac{e^{i\mathbf{k}\cdot(\mathbf{x}_2-\mathbf{x}_1)}}{(z^2-c^2\mathbf{k}^2+i\epsilon)}\right|au\right\rangle\frac{1}{[e_a-z-e_t(1-i\eta)]}\frac{1}{[e_b-z-e_u(1-i\eta')]}. \quad (2.22)$$

The integration over z leads to the integral

$$I = \int_{-\infty}^{\infty}\frac{dz}{2\pi}\frac{1}{(q-z+i\eta_t)}\frac{1}{(q'-z+i\eta_u)}\frac{1}{[z^2-(ck'-i\eta)^2]}\frac{1}{[z^2-(ck-i\eta)^2]}. \quad (2.23)$$

For positive values of the intermediate energies e_t and e_u, this integral becomes

$$I = \frac{i}{2ckck'(c^2k^2-c^2k'^2)}\left\{\frac{ck}{(q-ck')(q'-ck')}-\frac{ck'}{(q-ck)(q'-ck)}\right\} \quad (2.24)$$

and the corresponding energy contribution

$$\Delta E^{++}_{{\rm cro},tu} = -\left(\frac{e^2c^2}{\epsilon_0}\right)^2\int\frac{d^3\mathbf{k}}{(2\pi)^3}\int\frac{d^3\mathbf{k}'}{(2\pi)^3}\langle cu|\alpha^\nu_3\alpha_{\nu4}e^{i\mathbf{k}'\cdot(\mathbf{x}_3-\mathbf{x}_4)}|tb\rangle\langle td|\alpha^\mu_1\alpha_{\mu2}e^{i\mathbf{k}\cdot(\mathbf{x}_2-\mathbf{x}_1)}|au\rangle$$
$$\times\frac{1}{2ckck'(c^2k^2-c^2k'^2)}\left\{\frac{ck}{(q-ck')(q'-ck')}-\frac{ck'}{(q-ck)(q'-ck)}\right\}. \quad (2.25)$$

After the integration over the angular parts of the photon momenta we then get

$$\Delta E^{++}_{\rm cro} = -\left(\frac{e^2}{2\pi^2\epsilon_0}\right)^2 \sum_{l,l'}(2l+1)(2l'+1)\int dk\int dk'\sum_t\sum_u \langle c|\alpha^\nu \mathbf{C}^{l'} j_{l'}(k'r)|t\rangle\cdot\langle u|\alpha_\nu \mathbf{C}^{l'} j_{l'}(k'r)|b\rangle$$
$$\times\langle t|\alpha^\mu \mathbf{C}^{l} j_{l}(kr)|a\rangle\cdot\langle d|\alpha_\mu \mathbf{C}^{l} j_{l}(kr)|u\rangle \frac{ckck'}{2(ck+ck')}\left\{\frac{c^2k^2+c^2kk'+c^2k'^2-(q-q')(ck+ck')+qq'}{(q-ck)(q'-ck)(q-ck')(q'-ck')}\right\}. \quad (2.26)$$

Here the reference state is also left out of the summation over the intermediate states, although there is no singularity for crossed photons. However, there is a large cancellation between reference-state contributions for crossed and uncrossed photons. In the Feynman gauge there is even a contribution of order $Z\alpha$ hartree, which is canceled when the two diagrams are added [34,25]. In addition, there is a residual contribution of higher order, which will be treated in Appendix A.

So far we have considered only intermediate states with positive energy. The corresponding results for intermediate states of negative energy are obtained with the substitution

$$q\to -q \quad \text{and/or} \quad q'\to -q'. \quad (2.27)$$

By making both replacements, we get the results where both intermediate states have negative energy. By making one of the replacements (for q or q') we get, from the expression for uncrossed photons, the result for crossed photons where one of the states has negative energy and vice versa. There is also a change of the overall sign for each replacement.

C. Coulomb gauge

In the Coulomb gauge we have to replace the interaction in the Feynman gauge

$$-\alpha_1^\mu\alpha_{\mu 2}\frac{e^2c^2}{\epsilon_0}\int\frac{d^3\mathbf{k}}{(2\pi)^3}\frac{e^{i\mathbf{k}\cdot(\mathbf{x}_2-\mathbf{x}_1)}}{(z^2-c^2\mathbf{k}^2+i\epsilon)} \quad (2.28)$$

by the following three terms: (a) the unretarded Coulomb interaction (scalar)

$$-\frac{e^2c^2}{\epsilon_0}\int\frac{d^3\mathbf{k}}{(2\pi)^3}\frac{e^{i\mathbf{k}\cdot(\mathbf{x}_2-\mathbf{x}_1)}}{(-c^2\mathbf{k}^2+i\epsilon)}, \quad (2.29)$$

(b) the retarded Gaunt interaction (vector)

$$-\boldsymbol{\alpha}_1\cdot\boldsymbol{\alpha}_2\frac{e^2c^2}{\epsilon_0}\int\frac{d^3\mathbf{k}}{(2\pi)^3}\frac{e^{i\mathbf{k}\cdot(\mathbf{x}_2-\mathbf{x}_1)}}{(z^2-c^2\mathbf{k}^2+i\epsilon)}, \quad (2.30)$$

and the (c) scalar retardation

$$-\left[c\boldsymbol{\alpha}_1\cdot\boldsymbol{\nabla}_1,\left[c\,\boldsymbol{\alpha}_2\cdot\boldsymbol{\nabla}_2,\frac{e^2c^2}{\epsilon_0}\int\frac{d^3\mathbf{k}}{(2\pi)^3}\times\frac{e^{i\mathbf{k}\cdot(\mathbf{x}_2-\mathbf{x}_1)}}{(z^2-c^2\mathbf{k}^2+i\epsilon)(-c^2\mathbf{k}^2+i\epsilon)}\right]\right]. \quad (2.31)$$

If the orbitals are generated in a local potential, we can replace $c\boldsymbol{\alpha}\cdot\boldsymbol{\nabla}$ in the commutators by the imaginary unit times the single-electron Dirac Hamiltonian h_D, which generates the difference between the orbital energies (q or q') when acting on the orbitals. This gives the matrix element

$$\frac{e^2c^2}{\epsilon_0}qq'\left\langle tu\left|\int\frac{d^3\mathbf{k}}{(2\pi)^3}\frac{e^{i\mathbf{k}\cdot(\mathbf{x}_2-\mathbf{x}_1)}}{(z^2-c^2\mathbf{k}^2+i\epsilon)(-c^2\mathbf{k}^2+i\epsilon)}\right|ab\right\rangle, \quad (2.32)$$

where $q=e_a-e_t$ and $q'=e_b-e_u$.

1. Coulomb-Coulomb interactions

The combination of two unretarded Coulomb interactions leads to the z integral

$$i\int_{-\infty}^{\infty}\frac{dz}{2\pi}\frac{1}{(q-z+i\eta_t)}\frac{1}{(q'+z+i\eta_u)}\times\frac{1}{(-c^2k^2+i\eta)}\frac{1}{(-c^2k'^2+i\eta)}. \quad (2.33)$$

If the intermediate energies e_t and e_u are both positive, the integral becomes $1/(q+q')$ and if both are negative $-1/(q+q')$. If e_t and e_u have different signs, the integral vanishes. There is no contribution from crossed photons in this case.

2. Coulomb-Gaunt interactions

The z integral becomes, in this case for uncrossed photons,

$$i\int_{-\infty}^{\infty}\frac{dz}{2\pi}\frac{1}{(q-z+i\eta_t)}\frac{1}{(q'+z+i\eta_u)}\times\frac{1}{(z^2-c^2k^2+i\eta)}\frac{1}{(-c^2k'^2+i\eta)}, \quad (2.34)$$

which for positive intermediate energies becomes

$$\frac{(-2ck+q+q')}{2ck(q-ck)(q'-ck)(q+q')}\frac{1}{(-c^2k'^2)}. \quad (2.35)$$

For crossed photons the z integral becomes

$$i\int_{-\infty}^{\infty}\frac{dz}{2\pi}\frac{1}{(q-z+i\eta_t)}\frac{1}{(q'-z+i\eta_u)}\times\frac{1}{(z^2-c^2k^2+i\eta)}\frac{1}{(-c^2k'^2+i\eta)}, \quad (2.36)$$

which for positive intermediate energies becomes

$$\frac{1}{2ck(q-ck)(q'-ck)}\frac{1}{(-c^2k'^2)}. \tag{2.37}$$

3. Coulomb-scalar retardation

The z integral is, for uncrossed and crossed photons, the same as for the Coulomb-Gaunt interaction [Eqs. (2.35) and (2.37), respectively] times $-qq'/(ck)^2$. For crossed photons there is an additional sign change since the initial and final single-electronic states are exchanged for one of the interactions.

4. Gaunt-scalar retardation

The z integral is, for uncrossed and crossed photons, the same as in the Feynman gauge [Eqs. (2.13) and (2.24), respectively] times $-qq'/(ck)^2$. For crossed photons there is also an additional sign change.

5. Scalar retardation–scalar retardation

The z integral is, for uncrossed as well as crossed photons, the same as in the Feynman gauge [Eqs. (2.13) and (2.24), respectively] times $qq'/(ck)^2 \times qq'/(ck')^2$. The contributions for intermediate states with negative energy are obtained in the same way as in the Feynman gauge [see Eq. (2.27)]. This applies to all the combinations of interactions given in Secs. II C 2–II C 5 above.

D. Unretarded contributions

In order to be able to compare the QED results with those of standard RMBPT calculations, we have performed the calculations also without retardation. This is easily done in the formalism presented here simply by setting $z = 0$ in the photon propagators. Leaving out the effects of the virtual pairs then yields results which are exactly equivalent to the corresponding RMBPT results.

III. NUMERICAL PROCEDURE AND RESULTS

The basis functions used in this calculation are obtained by solving the single-particle Dirac equation in the nuclear potential (point nucleus), using the method of discretization, developed by Salomonson and Öster [12]. The radial integrals appearing here are identical to those appearing in the self-energy calculation [10] and have been evaluated in the same way. Analytical Bessel functions are used and the radial integrations are performed numerically. The integrations over the photon momenta are also performed numerically, as in our self-energy calculations, using the method of Gaussian quadrature. $70-150$ (in a few cases 200) grid points are used in the radial integrations and $50-75$ (in a few cases 90) points in the momentum integration. The angular factors needed are derived in Appendix B. Partial waves up to $L = 20$ have been evaluated, which is sufficient in order to perform a reliable L extrapolation.

The calculations have been performed for a number of nuclear charges, ranging from $Z = 2$ to $Z = 92$. The Coulomb gauge is generally used and in a few cases the Feynman gauge is also used in order to test the gauge invariance. In Tables I–III we show some results for $Z = 2, 10$, and 80 in the two gauges. Separate results are given here for the angular momenta L of the intermediate electronic states $L = 0-5$ as well as accumulated results for $L \leq 10$ and L-extrapolated values. Contributions nondiagonal in L, which are rather small, have been included here in the entry for the larger of the two L values. This means, for instance, that the s-d contribution is included in the entry for $L = 2$. Columns 3 and 4 show the results in the Feynman and the Coulomb gauges, respectively. Results are given separately for no virtual pairs with retardation (NVP) and for virtual pairs.

In the Coulomb gauge the Coulomb-Gaunt interaction and the Coulomb-scalar retardation (see Secs. II C 2 and II C 3) form together the Coulomb-Breit interaction. The Coulomb-Gaunt part is closely related to the corresponding part in the Feynman gauge, while the Coulomb-scalar retardation corresponds to the retardation of the Coulomb-Coulomb interaction in that gauge. The latter can be illustrated, for instance, by the $L = 0$ results for helium in Table I, where the Coulomb-scalar retardation result in the Coulomb gauge is 2.99 μhartree, which is very close to the difference between the Coulomb-Coulomb results of the two gauges (2.96 μhartree).

It should be noted that the scalar retardation term has a *frequency-independent* part, appearing in the frequency-independent Breit interaction. Normally only the effect of the *frequency dependence* of the Breit interaction (see Sec. II D) is referred to as the retardation and this is the convention we adopt in comparing our retarded and unretarded results in the Coulomb gauge in the tables.

The gauge invariance between the Coulomb and Feynman gauges is demonstrated numerically with high accuracy. The results we obtain in the two gauges agree to 9–10 figures. This is a demonstration of the accuracy of the k integration. (Identical radial integrals are used in the two calculations.) For each photon interaction we have separated out the scalar (A0) and the vector (ALF) parts of $\alpha_\mu\alpha^\mu = 1 - \boldsymbol{\alpha}\cdot\boldsymbol{\alpha}$. As can be seen from the tables, the gauge invariance is valid separately for the scalar-scalar (A0-A0), scalar-vector (A0-ALF), and vector-vector (ALF-ALF) parts of the two-photon interaction. The gauge invariance holds also for the individual L, even for high Z, with the same degree of accuracy.

The contribution from the crossed photons are listed separately. It is well known that this contribution is much larger in the Feynman gauge than in the Coulomb gauge [28,29], which caused the apparent gauge dependence in RMBPT, where crossed photons are not included. For $Z = 10$ the crossed-photon contribution is about 100 times larger in the Feynman gauge and for $Z = 2$ about

TABLE I. Two-photon contributions for the ground state of the helium atom, using Feynman and Coulomb gauges (in μhartree). The reference state contribution is not included in this table. The unretarded results are compared with relativistic many-body calculations with unretarded Breit interaction (RMBPT) taken from the work of Blundell, Mohr, Johnson, and Sapirstein [9,35–37]. The abbreviations NVP for no virtual pairs and VP for virtual pairs are used.

L	Contribution	Feynman	Coulomb	Unretarded	RMBPT
0	Coulomb-Coulomb NVP	-125 353.14	-125 356.10	-125 356.10	-125 356.11
	Coulomb-Gaunt NVP	-68.11	-68.16	-68.28	-68.28
	Coulomb-retardation NVP		2.99	3.11	3.11
	Breit-Breit NVP	-0.02	-0.01	-0.01	
	Total NVP	-125 421.27	-125 421.29	-125 421.29	
	Virtual pairs	-0.06	-0.04		
	Total	-125 421.3284	-125 421.3284	-125 421.29	
1	Coulomb-Coulomb NVP	-26 481.45	-26 492.41	-26 492.41	-26 492.41
	Coulomb-Gaunt NVP	-43.11	-43.43	-45.59	-45.59
	Coulomb-retardation NVP		11.04	11.92	11.93
	Breit-Breit NVP	-0.03	-0.02	-0.02	
	Total NVP	-26 524.60	-26 524.82	-26 526.09	
	Virtual pairs	-0.47	-0.25		
	Total	-26 525.0729	-26 525.0729	-26 526.09	
2	Coulomb-Coulomb NVP	-3 901.55	-3 904.66	-3 904.66	-3 904.65
	Coulomb-Gaunt NVP	-10.94	-11.06	-11.35	-11.35
	Coulomb-retardation NVP		3.15	3.36	3.36
	Breit-Breit NVP	-0.02	-0.01	-0.01	
	Total NVP	-3 912.51	-3 912.58	-3 912.66	
	Virtual pairs	-0.20	-0.13		
	Total	-3 912.7106	-3 912.7106	-3 912.66	
3	Coulomb-Coulomb NVP	-1 075.45	-1 076.94	-1 076.94	-1 076.93
	Coulomb-Gaunt NVP	-5.06	-5.13	-5.30	-5.29
	Coulomb-retardation NVP		1.52	1.65	1.65
	Breit-Breit NVP	-0.02	-0.01	-0.01	
	Total NVP	-1 080.53	-1 080.57	-1 080.60	
	Virtual pairs	-0.12	-0.09		
	Total	-1 080.6572	-1 080.6572	-1 080.60	
4	Coulomb-Coulomb NVP	-404.76	-405.62	-405.62	-405.62
	Coulomb-Gaunt NVP	-2.91	-2.97	-3.08	-3.07
	Coulomb-retardation NVP		0.89	0.98	0.98
	Breit-Breit NVP	-0.02	-0.01	-0.01	
	Total NVP	-407.69	-407.71	-407.73	
	Virtual pairs	-0.09	-0.07	0.00	
	Total	-407.7761	-407.7761	-407.73	
5	Coulomb-Coulomb NVP	-184.12	-184.68	-184.68	-184.67
	Coulomb-Gaunt NVP	-1.89	-1.93	-2.01	-2.01
	Coulomb-retardation NVP		0.58	0.65	0.65
	Breit-Breit NVP	-0.01	-0.01	-0.01	
	Total NVP	-186.02	-186.04	-186.05	
	Virtual pairs	-0.07	-0.05		
	Total	-186.0899	-186.0899	-186.05	
≤ 10	Coulomb-Coulomb NVP	-157 617.50	-157 638.62	-157 638.62	-157 638.51
	Coulomb-Gaunt NVP	-136.08	-136.85	-140.03	-139.97
	Coulomb-retardation NVP		21.38	23.12	23.10
	Breit-Breit NVP	-0.18	-0.09	-0.11	
	Total NVP	-157 753.75	-157 754.18	-157 755.64	
	Virtual pairs	-1.23	-0.81		
	Total	-157 754.9873	-157 754.9873	-157 755.64	
		Extrapolated total			
	Coulomb-Coulomb NVP	-157 659.55	-157 681.52	-157 681.52	-157 681.47

TABLE I. *(Continued.)*

L	Contribution	Feynman	Coulomb	Unretarded	RMBPT
	Coulomb-Gaunt NVP	-139.29	-140.25	-143.87	-144.46
	Coulomb-retardation NVP		22.30	24.39	24.59
	Breit-Breit NVP	-0.34	-0.17	-0.22	
	Total NVP	-157 799.18	-157 799.65	-157 801.22	
	VP single Coulomb-Coulomb		0.18		
	VP single Coulomb-Breit		-0.63		
	VP single Breit-Breit		0.28		
	VP single total	-0.01	-0.17		
	VP double Coulomb-Coulomb		0.00		
	VP double Breit-Coulomb		-0.06		
	VP double Breit-Breit		-0.95		
	VP double total	-1.64	-1.02		
	VP total	-1.65	-1.19		
	A0-A0	-157 659.40	-157 659.40	-157 657.18	
	A0-ALF	-139.92	-139.92	-143.56	
	ALF-ALF	-1.53	-1.53	-0.47	
	Coulomb-Coulomb total		-157 681.35	-157 681.52	
	Coulomb-Breit total		-118.64	-119.48	
	Breit-Breit total		-0.85	-0.22	
	Grand total	-157 800.8477	-157 800.8477	-157 801.22	
		Crossed photons			
	Coulomb-Coulomb				
	No virtual pair	-1 659.31	0		
	Virtual pairs	0.08	0.18		
	Total	-1 659.23	0.18		
	Coulomb-Breit				
	No virtual pair	-0.43	-0.96		
	Virtual pairs	-0.16	-0.38		
	Total	-0.59	-1.34		
	Breit-Breit				
	No virtual pair	0.03	0.00		
	Virtual pairs	0.55	0.09		
	Total	0.58	0.10		
	Total				
	No virtual pair	-1 659.71	-0.95		
	single pair	-0.30	-0.18		
	Double pairs	0.77	0.08		
	Total pair	0.46	-0.11		
	Grand total	-1 659.25	-1.06		

1600 times larger.

In the fifth column of Tables I–III we give the unretarded results in the Coulomb gauge, i.e., discarding retardation and virtual-pair effects. These values should be exactly equivalent to RMBPT calculations and for $Z = 2$ and $Z = 10$ a comparison is made with the available RMBPT results of Johnson *et al.* [9,35–37]. The agreement here is remarkably good, which also serves as a test of the accuracy of the radial integrations. The contribution from the reference state is not included in these tables, but is separately given in Table IV.

In Table V the Coulomb-gauge results for all Z values considered in this work are summarized. Again the unretarded results correspond to a many-body calculation, omitting retardation and virtual-pair effects. "No virtual pairs" represents the value *with* retardation, but with no virtual-pair effect. Thus the difference between the unretarded and no virtual pairs results represents the effect of *retardation.* The virtual-pair effect, separated into single and double pairs, is given separately. We have also included the contribution from the reference state, given in Table IV. "Grand total" represents the entire two-photon exchange effect and "QED" is the part not included in a many-body calculation, i.e., the difference between the total effect and the unretarded result. The first part of Table V represents the entire effect, i.e., non-crossed and crossed photons. The separate contributions of the crossed photons are displayed in the second part of the

TABLE II. Same as Table I, but for heliumlike neon. The contributions are in μhartree.

L	Contribution	Feynman	Coulomb	Unretarded	RMBPT
0	Coulomb-Coulomb NVP	-125 833.89	-125 895.77	-125 895.77	-125 895.77
	Coulomb-Gaunt NVP	-1 680.90	-1 686.29	-1 699.11	-1 699.11
	Coulomb-retardation NVP		63.87	75.45	75.45
	Breit-Breit NVP	-8.74	-7.02	-7.81	
	Total NVP	-127 523.53	-127 525.21	-127 527.25	
	Virtual pairs	-9.44	-7.76		
	Total	-127 532.9645	-127 532.9645	-127 527.25	
1	Coulomb-Coulomb NVP	-26 217.33	-26 430.65	-26 430.65	-26 430.65
	Coulomb-Gaunt NVP	-915.99	-947.63	-1 116.10	-1 116.09
	Coulomb-retardation NVP		220.59	291.41	291.41
	Breit-Breit NVP	-14.76	-8.37	-10.68	
	Total NVP	-27 148.08	-27 166.05	-27 266.02	
	Virtual pairs	-47.88	-29.90		
	Total	-27 195.9593	-27 195.9593	-27 266.02	
2	Coulomb-Coulomb NVP	-3 815.85	-3 872.78	-3 872.78	-3 872.78
	Coulomb-Gaunt NVP	-227.40	-238.20	-266.16	-266.14
	Coulomb-retardation NVP		60.09	78.55	78.54
	Breit-Breit NVP	-7.03	-3.77	-4.99	
	Total NVP	-4 050.28	-4 054.66	-4 065.39	
	Virtual pairs	-20.17	-15.78		
	Total	-4 070.4432	-4 070.4432	-4 065.39	
3	Coulomb-Coulomb NVP	-1 036.35	-1 061.06	-1 061.06	-1 061.05
	Coulomb-Gaunt NVP	-98.33	-104.13	-118.06	-118.02
	Coulomb-retardation NVP		26.49	36.68	36.67
	Breit-Breit NVP	-4.75	-2.50	-3.48	
	Total NVP	-1 139.43	-1 141.19	-1 145.92	
	Virtual pairs	-12.10	-10.33		
	Total	-1 151.5241	-1 151.5241	-1 145.92	
4	Coulomb-Coulomb NVP	-383.60	-396.64	-396.64	-396.64
	Coulomb-Gaunt NVP	-52.69	-56.35	-65.06	-65.02
	Coulomb-retardation NVP		14.17	20.73	20.72
	Breit-Breit NVP	-3.51	-1.83	-2.66	
	Total NVP	-439.80	-440.66	-443.64	
	Virtual pairs	-8.31	-7.45		
	Total	-448.1096	-448.1096	-443.64	
5	Coulomb-Coulomb NVP	-171.44	-179.14	-179.14	-179.14
	Coulomb-Gaunt NVP	-31.77	-34.28	-40.28	-40.23
	Coulomb-retardation NVP		8.46	13.01	12.99
	Breit-Breit NVP	-2.70	-1.41	-2.12	
	Total NVP	-205.90	-206.36	-208.52	
	Virtual pairs	-6.12	-5.67	0.00	
	Total	-212.0261	-212.0261	-208.52	
≤ 10	Coulomb-Coulomb NVP	-157 653.09	-158 044.08	-158 044.08	-158 044.02
	Coulomb-Gaunt NVP	-3 065.20	-3 130.71	-3 382.54	-3 382.04
	Coulomb-retardation NVP		408.72	541.32	541.16
	Breit-Breit NVP	-48.90	-28.78	-38.00	
	Total NVP	-160 767.19	-160 794.84	-160 923.30	
	Virtual pairs	-120.04	-92.39		
	Total	-160 887.2335	-160 887.2334	-160 923.30	
		Extrapolated total			
	Coulomb-Coulomb NVP	-157 686.86	-158 083.24	-158 083.24	-158 083
	Coulomb-Gaunt NVP	-3 092.60	-3 162.57	-3 425.16	
	Coulomb-retardation NVP		415.21	555.48	-2 870
	Breit-Breit NVP	-56.68	-32.98	-46.01	-46

TABLE II. *(Continued.)*

L	Contribution	Feynman	Coulomb	Unretarded	RMBPT
	Total NVP	-160 836.10	-160 863.25	-160 998.69	-160 999
	VP single Coulomb-Coulomb		26.63		
	VP single Coulomb-Breit		-87.57		
	VP single Breit-Breit		42.17		
	VP single total	8.99	-18.82		
	VP double Coulomb-Coulomb		-1.36		
	VP double Breit-Coulomb		-13.28		
	VP double Breit-Breit		-76.09		
	VP double total	-145.67	-90.73		
	VP total	-136.68	-109.55		
	A0-A0	-157 667.48	-157 667.48	-157 535.91	
	A0-ALF	-3 176.97	-3 176.97	-3 374.50	
	ALF-ALF	-128.22	-128.22	-88.48	
	Coulomb-Coulomb total		-158 057.99	-158 083.24	
	Coulomb-Breit total		-2 847.78	-2 869.67	
	Breit-Breit total		-66.88	-46.01	
	Grand total	-160 972.6487	-160 972.6486	-160 998.69	-160 999
		Crossed photons			
	Coulomb-Coulomb				
	No virtual pair	-7 262.93	0		
	Virtual pairs	10.87	26.63		
	Total	-7 252.07	26.63		
	Coulomb-Breit				
	No virtual pair	-39.72	-66.06		
	Virtual pairs	-21.24	-54.95		
	Total	-60.96	-121.01		
	Breit-Breit				
	No virtual pair	5.21	0.58		
	Virtual pairs	33.72	9.25		
	Total	38.93	9.83		
	Total				
	No virtual pair	-7 297.40	-65.34		
	single pair	-37.35	-25.12		
	Double pairs	60.70	6.65		
	Total pair	23.35	-18.77		
	Grand total	-7 274.06	-84.11		

table. The numerical uncertainty of the calculations presented here is estimated to be of the order of 0.1 μhartree for low Z and increasing to one or a few microhartrees for high Z.

When available, we have, in Table V, also included the results of Blundell *et al.* [9] for the entire two-photon contribution as well as for the QED correction. It should be noted that our calculations are primarily performed with a *point* nucleus, while Blundell *et al.* use an *extended* nucleus. For low Z, where the effect of the nuclear extension is negligible, the agreement between the two calculations is very good. For instance, for $Z = 10$, Blundell *et al.* obtain a total two-photon contribution of $-0.160\,972$ hartree and a RMBPT result of $-0.160\,999$ hartree, giving a QED correction of 0.000 026 hartree. Our corresponding results are, for the two-photon contribution, $-0.160\,972\,6$ hartree, compared to the unretarded (RMBPT) result of $-0.160\,998\,7$ hartree giving a QED correction of 0.000 026 2 hartree.

In order to estimate the nuclear-size effect for large Z, we have performed calculations also with an extended nucleus (uniformly charged) for $Z = 54$, 80, and 92. The results are shown in Table V. The effect of the extended nucleus increases drastically for high Z from 44 μhartree for $Z = 54$ to about 2500 μhartree for $Z = 92$. Most of that effect is present also in the unretarded contribution, i.e., in a standard many-body calculation. The residual QED effect, which is of more interest, is consequently considerably smaller, about -2 μhartree for $Z = 54$ and about -280 μhartree for $Z = 92$. For $Z = 80$ we can compare our results with those of Blundell *et al.* We obtain a total two-photon effect of $-0.381\,263$ hartree and

TABLE III. Same as Table I, but for heliumlike mercury. The contributions are in μhartree.

L	Contribution	Feynman	Coulomb	Unretarded
0	Coulomb-Coulomb NVP	-179 760	-181 510	-181 510
	Coulomb-Gaunt NVP	-110 131	-111 376	-113 694
	Coulomb-retardation NVP		1 958	3 679
	Breit-Breit NVP	-15 590	-14 590	-17 952
	Total NVP	-305 481	-305 518	-309 477
	Virtual pairs	-3 619	-3 582	
	Total	-309 099.5511	-309 099.5512	-309 477
1	Coulomb-Coulomb NVP	-21 736	-25 979	-25 979
	Coulomb-Gaunt NVP	-24 310	-28 644	-51 020
	Coulomb-retardation NVP		4 944	13 665
	Breit-Breit NVP	-13 637	-8 419	-16 164
	Total NVP	-59 683	-58 099	-79 498
	Virtual pairs	-1 037	-2 621	
	Total	-60 719.4636	-60 719.4637	-79 498
2	Coulomb-Coulomb NVP	-2 730	-3 584	-3 584
	Coulomb-Gaunt NVP	-4 094	-4 936	-7 687
	Coulomb-retardation NVP		989	2 467
	Breit-Breit NVP	-2 546	-1 566	-2 910
	Total NVP	-9 370	-9 097	-11 714
	Virtual pairs	428	155	
	Total	-8 942.0446	-8 942.0446	-11 714
3	Coulomb-Coulomb NVP	-715	-1 006	-1 006
	Coulomb-Gaunt NVP	-1 338	-1 628	-2 513
	Coulomb-retardation NVP		344	872
	Breit-Breit NVP	-883	-533	-1 063
	Total NVP	-2 936	-2 824	-3 710
	Virtual pairs	-296	-408	
	Total	-3 232.2869	-3 232.2869	-3 710
4	Coulomb-Coulomb NVP	-269	-397	-397
	Coulomb-Gaunt NVP	-588	-720	-1 116
	Coulomb-retardation NVP		156	403
	Breit-Breit NVP	-404	-241	-504
	Total NVP	-1 261	-1 203	-1 615
	Virtual pairs	-224	-283	
	Total	-1 485.6871	-1 485.6871	-1 615
5	Coulomb-Coulomb NVP	-125	-192	-192
	Coulomb-Gaunt NVP	-308	-378	-590
	Coulomb-retardation NVP		83	218
	Breit-Breit NVP	-217	-129	-278
	Total NVP	-650	-616	-843
	Virtual pairs	-152	-186	
	Total	-802.0966	-802.0966	-843
≤ 10	Coulomb-Coulomb NVP	-205 496	-212 930	-212 930
	Coulomb-Gaunt NVP	-141 233	-148 257	-177 527
	Coulomb-retardation NVP		8 601	21 647
	Breit-Breit NVP	-33 619	-25 678	-39 327
	Total NVP	-380 348	-378 264	-408 137
	Virtual pairs	-5 205	-7 289	
	Total	-385 553.0750	-385 553.0749	-408 137
		Extrapolated total		
	Coulomb-Coulomb NVP	-205 543	-213 015	-213 015
	Coulomb-Gaunt NVP	-141 408	-148 476	-177 881
	Coulomb-retardation NVP		8 651	21 781
	Breit-Breit NVP	-33 759	-25 759	-39 524
	Total NVP	-380 709	-378 599	-408 640
	VP single Coulomb-Coulomb		8 092	

TABLE III. *(Continued.)*

L	Contribution	Feynman	Coulomb	Unretarded
	VP single Coulomb-Breit		-14 233	
	VP single Breit-Breit		15 653	
	VP single total	22 858	9 513	
	VP double Coulomb-Coulomb		-928	
	VP double Breit-Coulomb		-5 316	
	VP double Breit-Breit		-10 752	
	VP double total	-28 230	-16 996	
	VP total	-5 371	-7 483	
	A0-A0	-200 426	-200 426	-194 388
	A0-ALF	-157 190	-157 190	-156 533
	ALF-ALF	-28 469	-28 469	-57 717
	Coulomb-Coulomb total		-205 852	-213 015
	Coulomb-Breit total		-159 376	-156 100
	Breit-Breit total		-20 857	-39 524
	Grand total	-386 084.1292	-386 084.1284	-408 640
		Crossed photons		
	Coulomb-Coulomb			
	No virtual pair	-36 707	0	
	Virtual pairs	3 375	8 092	
	Total	-33 332	8 092	
	Coulomb-Breit			
	No virtual pair	-12 394	-9 302	
	Virtual pairs	-807	-8 093	
	Total	-13 201	-17 395	
	Breit-Breit			
	No virtual pair	2 030	1 349	
	Virtual pairs	14 874	4 396	
	Total	16 904	5 745	
	Total			
	No virtual pair	-47 071	-7 953	
	single pair	9 888	4 053	
	Double pairs	7 554	342	
	Total pair	17 442	4 395	
	Grand total	-29 630	-3 558	

a QED effect of 0.026 657 hartree, compared with the result −0.381 28 hartree and 0.026 64 hartree, respectively, of Blundell *et al.*

IV. ANALYSIS

The various energy contributions to heliumlike ions of orders $(Z\alpha)^3$ and $(Z\alpha)^3\ln(\alpha)$ have been evaluated analytically by Kabir and Salpeter [5], Araki [30], Sucher [6], Ermolaev [38], and others. Kabir and Salpeter [5] evaluated the leading contributions due to the exchange of two transverse photons between the electrons of neutral helium. They found that there is a contribution of order $(Z\alpha)^3\ln(\alpha)$ in the exchange of two transverse photons due to the virtual pairs, which for neutral helium becomes

$$\Delta E_{\rm KS} = 2\alpha^3 \ln\alpha \langle\delta(\mathbf{r}_{12})\rangle. \tag{4.1}$$

Araki [30] and Sucher [6] have evaluated also the $(Z\alpha)^3$ terms and the results of Sucher are summarized in Ta-

TABLE IV. The reference-state contribution for the ground state in He-like ions using both an extended and a point nucleus (in μhartree). The numbers in brackets denote multiplication by powers of 10.

Ion	$R_{\rm rms}$ (fm)	Extended nucleus	Point nucleus
$_{2}$He			3.71390[-5]
$_{4}$Be			1.18862[-3]
$_{6}$C			9.02822[-3]
$_{10}$Ne			1.16192[-1]
$_{14}$Si			6.25630[-1]
$_{18}$Ar			2.20146[0]
$_{24}$Cr			9.30539[0]
$_{30}$Zn			2.85114[1]
$_{36}$Kr	4.230	7.12913[1]	7.12985[1]
$_{42}$Mo			1.55030[2]
$_{48}$Cd			3.04407[2]
$_{54}$Xe	4.826	5.52862[2]	5.53110[2]
$_{60}$Nd	4.915	9.45067[2]	9.45709[2]
$_{70}$Yb	5.273	2.08079[3]	2.08379[3]
$_{80}$Hg	5.475	4.15025[3]	4.16224[3]
$_{92}$U	5.860	8.63316[3]	8.69358[3]

TABLE V. Summary of two-photon contributions for heliumlike systems (in μhartree).

Contribution	Nuclear charge	2	4	6	10
		Noncrossing and crossing photons			
Coulomb-Coulomb					
Unretarded	-157 681.52	-157 728.47	-157 809.52	-158 083.24	
single pair		0.18	1.78	5.97	26.63
Double pairs		0.00	-0.06	-0.25	-1.36
Total pair		0.18	1.72	5.72	25.23
Total		-157 681.35	-157 726.77	-157 803.78	-158 057.99
Coulomb-Breit					
Unretarded		-119.48	-473.34	-1 054.15	-2 869.67
No virtual pair		-117.96	-462.88	-1 022.78	-2 747.36
Retardation		1.52	10.46	31.37	122.32
Single pair		-0.63	-6.01	-19.96	-87.57
Double pairs		-0.06	-0.77	-2.74	-13.28
Total pair		-0.69	-6.78	-22.69	-100.85
Total		-118.64	-469.61	-1 045.44	-2 847.78
Breit-Breit					
Unretarded		-0.22	-2.42	-8.93	-46.01
No virtual pair		-0.17	-1.77	-6.43	-32.98
Retardation		0.05	0.64	2.50	13.04
Single pair		0.28	2.67	9.13	42.17
Double pairs		-0.95	-6.62	-19.77	-76.09
Total pair		-0.67	-3.95	-10.64	-33.92
Reference state		0.00	0.00	0.01	0.12
Total		-0.85	-5.72	-17.05	-66.76
Total					
Unretarded		-157 801.22	-158 204.16	-158 872.49	-160 998.69
No virtual pair		-157 799.65	-158 193.12	-158 838.72	-160 863.25
Retardation		1.57	11.04	33.77	135.44
Single pair		-0.17	-1.55	-4.85	-18.82
Double pairs		-1.02	-7.46	-22.72	-90.73
Total pair		-1.19	-9.01	-27.57	-109.56
Grand total		-157 800.85	-158 201.99	-158 866.29	-160 972.53
Unretarded		-157 801.22	-158 204.16	-158 872.49	-160 998.69
QED=total−unretarded		0.38	2.18	6.20	26.16
Grand total extended nucleus					
Unretarded extended nucleus					
QED extended nucleus					
Blundell *et al.* extended nucleus [9]					
Grand total					-160 972
QED					26
		Crossing photons			
Coulomb-Coulomb					
No virtual pair		0	0	0	0
Virtual pairs		0.18	1.78	5.97	26.67
Total		0.18	1.78	5.97	26.67
Coulomb-Breit					
No virtual pair		-0.96	-6.25	-17.99	-66.06
Virtual pairs		-0.38	-3.78	-12.55	-54.95
Total		-1.34	-10.03	-30.54	-121.01

TABLE V. *(Continued).*

Contribution \ Nuclear charge	2	4	6	10
Breit-Breit				
No virtual pair	0.00	0.01	0.07	0.58
Virtual pairs	0.09	0.71	2.25	9.25
Total	0.10	0.72	2.31	9.83
Total				
No virtual pair	-0.95	-6.24	-17.93	-65.34
Single pair	-0.18	-1.76	-5.86	-25.12
Double pairs	0.08	0.48	1.52	6.65
Total pair	-0.11	-1.28	-4.33	-18.77
Grand total	-1.06	-7.52	-22.26	-84.11

Contribution \ Nuclear charge	14	18	24	30
Noncrossing and crossing photons				
Coulomb-Coulomb				
Unretarded	-158 520.29	-159 138.0	-160 442.4	-162 257.5
Single pair	69.40	140.0	309.6	567.1
Double pairs	-3.98	-8.5	-20.6	-40.7
Total pair	65.42	131.5	289.0	526.3
Total	-158 454.93	-159 006.5	-160 153.6	-161 731.5
Coulomb-Breit				
Unretarded	-5 515.00	-8 946.8	-15 491.0	-23 629.1
No virtual pair	-5 222.03	-8 393.7	-14 368.9	-21 719.9
Retardation	292.97	553.1	1 122.1	1 909.2
Single pair	-225.13	-446.9	-960.8	-1 703.1
Double pairs	-36.28	-75.8	-175.6	-334.4
Total pair	-261.40	-522.7	-1 136.4	-2 037.6
Total	-5 483.69	-8 917.1	-15 506.0	-23 758.3
Breit-Breit				
Unretarded	-136.37	-307.9	-785.9	-1 625.8
No virtual pair	-96.88	-216.8	-545.7	-1 114.7
Retardation	39.49	91.1	240.2	511.1
Single pair	114.00	237.5	545.8	1 031.8
Double pairs	-181.00	-341.3	-693.9	-1 186.5
Total pair	-67.00	-103.8	-148.1	-154.7
Reference state	0.63	2.2	9.3	28.5
Total	-163.31	-318.4	-684.5	-1 241.0
Total				
Unretarded	-164 171.89	-168 393.9	-176 719.9	-187 512.4
No virtual pair	-163 839.43	-167 748.5	-175 356.9	-185 091.8
Retardation	332.46	645.4	1 363.0	2 420.6
Single pair	-41.73	-69.6	-105.4	-104.3
Double pairs	-221.24	-425.5	-890.0	-1 561.1
Total pair	-262.97	-495.1	-995.3	-1 665.4
Grand total	-164 101.74	-168 242.0	-176 344.0	-186 730.5
Unretarded	-164 171.89	-168 393.9	-176 719.9	-187 512.4
QED=total−unretarded	70.15	151.9	376.0	781.9
Grand total extended nucleus				
Unretarded extended nucleus				
QED extended nucleus				
Blundell *et al.* extended nucleus [9]				
Grand total				-186 730
QED				780

TABLE V. *(Continued).*

Contribution \ Nuclear charge	14	18	24	30
	Crossing photons			
Coulomb-Coulomb				
No virtual pair	0	0	0	0
Virtual pairs	69.40	140.0	309.6	567.1
Total	69.40	140.0	309.6	567.1
Coulomb-Breit				
No virtual pair	-151.51	-278.7	-554.9	-939.7
Virtual pairs	-139.92	-275.4	-586.0	-1 029.3
Total	-291.43	-554.1	-1 140.9	-1 969.0
Breit-Breit				
No virtual pair	2.34	6.5	20.0	46.4
Virtual pairs	22.87	44.4	94.7	173.0
Total	25.21	50.8	114.7	219.4
Total				
No virtual pair	-149.16	-272.2	-534.9	-893.2
Single pair	-64.32	-124.4	-252.0	-410.7
Double pairs	16.67	33.2	70.4	121.6
Total pair	-47.65	-91.3	-181.7	-289.2
Grand total	-196.81	-363.5	-716.5	-1 182.3

Contribution \ Nuclear charge	36	42	48	54
	Noncrossing and crossing photons			
Coulomb-Coulomb				
Unretarded	-164 655.5	-167 722.6	-171 565	-176 315
Single pair	924.6	1 394.1	1 988	2 723
Double pairs	-71.5	-115.3	-175	-254
Total pair	853.1	1 278.8	1 813	2 468
Total	-163 802.9	-166 444.4	-169 752	-173 848
Coulomb-Breit				
Unretarded	-33 302.5	-44 489.7	-57 209	-71 521
No virtual pair	-30 393.0	-40 372.1	-51 684	-64 396
Retardation	2 909.4	4 117.6	5 525	7 125
Single pair	-2 673.9	-3 860.5	-5 241	-6 786
Double pairs	-562.9	-871.4	-1 269	-1 766
Total pair	-3 236.7	-4 731.9	-6 511	-8 552
Total	-33 629.9	-45 104.3	-58 195	-72 949
Breit-Breit				
Unretarded	-2 943.3	-4 856.1	-7 487	-10 966
No virtual pair	-1 995.0	-3 259.8	-4 986	-7 254
Retardation	948.3	1 596.3	2 501	3 711
Single pair	1 725.1	2 651.4	3 837	5 306
Double pairs	-1 820.4	-2 595.9	-3 510	-4 562
Total pair	-95.3	55.5	327	744
Reference state	71.3	155.0	304	553
Total	-2 019.5	-3 048.5	-4 353	-5 956
Total				
Unretarded	-200 901.2	-217 068.0	-236 260	-258 800
No virtual pair	-197 042.2	-211 356.2	-228 236	-247 967
Retardation	3 858.9	5 711.8	8 024	10 833
Single pair	-24.2	185.8	585	1 244
Double pairs	-2 454.7	-3 582.3	-4 954	-6 582
Total pair	-2 478.9	-3 396.5	-4 369	-5 338

TABLE V. *(Continued).*

Contribution \ Nuclear charge	36	42	48	54
Grand total	-199 451.9	-214 596.8	-232 300	-252 752
Unretarded	-200 901.2	-217 068.0	-236 260	-258 800
QED=total−unretarded	1 449.3	2 471.2	3 960	6 048
Grand total extended nucleus				-252 708
Unretarded extended nucleus				-258 754
QED extended nucleus				6 046
Blundell *et al.* extended nucleus [9]				
Grand total				
QED				
	Crossing photons			
Coulomb-Coulomb				
No virtual pair	0	0	0	0
Virtual pairs	924.6	1 394.1	1 988	2 723
Total	924.6	1 394.1	1 988	2 723
Coulomb-Breit				
No virtual pair	-1 439.7	-2 060.6	-2 809	-3 693
Virtual pairs	-1 602.9	-2 297.3	-3 098	-3 986
Total	-3 042.6	-4 357.9	-5 907	-7 678
Breit-Breit				
No virtual pair	90.6	156.8	250	373
Virtual pairs	289.4	458.3	698	1 033
Total	380.0	615.1	948	1 406
Total				
No virtual pair	-1 348.9	-1 903.8	-2 560	-3 319
Single pair	-572.8	-698.1	-735	-617
Double pairs	184.0	253.2	323	387
Total pair	-388.8	-444.9	-411	-230
Grand total	-1 737.7	-2 348.7	-2 971	-3 549

Contribution \ Nuclear charge	60	70	80	92
	Noncrossing and crossing photons			
Coulomb-Coulomb				
Unretarded	-182 148	-194 928	-213 015	-246 022
Single pair	3 615	5 521	8 092	12 443
Double pairs	-356	-590	-928	-1 531
Total pair	3 259	4 931	7 164	10 912
Total	-178 890	-189 998	-205 852	-235 110
Coulomb-Breit				
Unretarded	-87 536	-118 517	-156 100	-213 572
No virtual pair	-78 624	-106 205	-139 825	-191 655
Retardation	8 912	12 312	16 275	21 917
Single pair	-8 456	-11 385	-14 233	-16 912
Double pairs	-2 371	-3 649	-5 316	-7 943
Total pair	-10 827	-15 034	-19 549	-24 855
Total	-89 452	-121 240	-159 376	-216 513
Breit-Breit				
Unretarded	-15 429	-25 474	-39 524	-63 366
No virtual pair	-10 153	-16 658	-25 759	-41 280

TABLE V. *(Continued).*

Contribution \ Nuclear charge	60	70	80	92
Retardation	5 276	8 815	13 765	22 087
Single pair	7 084	10 814	15 653	23 292
Double pairs	-5 750	-8 043	-10 752	-14 656
Total pair	1 333	2 770	4 900	8 637
Reference state	946	2 084	4 162	8 694
Total	-7 873	-11 803	-16 695	-23 948
Total				
Unretarded	-285 114	-338 921	-408 640	-522 961
No virtual pair	-270 925	-317 791	-378 599	-478 955
Retardation	14 189	21 130	30 041	44 006
Single pair	2 244	4 950	9 513	18 824
Double pairs	-8 478	-12 282	-16 996	-24 129
Total pair	-6 233	-7 332	-7 483	-5 305
Grand total	-276 214	-323 040	-381 922	-475 570
Unretarded	-285 114	-338 921	-408 640	-522 961
QED=Total=Unretarded	8 900	15 880	26 718	47 391
Grand total extended nucleus			-381 263	-473 113
Unretarded extended nucleus			-407 919	-520 224
QED extended nucleus			26 656	47 112
Blundell *et al.* extended nucleus [9]				
Grand total	-276 140	-322 830	-381 280	
QED	8 890	15 850	26 640	
	Crossing photons			
Coulomb-Coulomb				
No virtual pair	0	0	0	0
Virtual pairs	3 615	5 521	8 092	12 443
Total	3 615	5 521	8 092	12 443
Coulomb-Breit				
No virtual pair	-4 718	-6 771	-9 302	-13 090
Virtual pairs	-4 935	-6 569	-8 093	-9 340
Total	-9 654	-13 340	-17 395	-22 430
Breit-Breit				
No virtual pair	531	880	1 349	2 083
Virtual pairs	1 491	2 624	4 396	7 752
Total	2 022	3 504	5 745	9 835
Total				
No virtual pair	-4 187	-5 891	-7 953	-11 006
Single pair	-264	1 122	4 053	10 943
Double pairs	435	454	342	-90
Total pair	171	1 576	4 395	10 855
Grand total	-4 016	-4 315	-3 558	-152

ble VI. Araki gives the following total contributions for the Coulomb-Coulomb, Coulomb-Breit, and Breit-Breit interactions, respectively (we are omitting the factor α^3 below):

$$-\frac{4}{3}\langle\delta(\mathbf{r}_{12})\rangle, \tag{4.2a}$$

$$\frac{4}{3}\left(\frac{8}{3}-2\ln\alpha\right)\langle\delta(\mathbf{r}_{12})\rangle-\frac{4}{3}\langle\boldsymbol{\sigma}_1\cdot\boldsymbol{\sigma}_2\delta(\mathbf{r}_{12})\rangle -\frac{8}{3}Q-\frac{2}{3\pi}M', \tag{4.2b}$$

$$\left(\frac{17}{3}-\frac{8}{3}\ln 2+2\ln\alpha\right)\langle\delta(\mathbf{r}_{12})\rangle +\frac{1}{3}\langle\boldsymbol{\sigma}_1\cdot\boldsymbol{\sigma}_2\delta(\mathbf{r}_{12})\rangle-2Q, \tag{4.2c}$$

which give the *total contribution*

$$\left(\frac{71}{9}-\frac{8}{3}\ln 2-\frac{2}{3}\ln\alpha\right)\langle\delta(\mathbf{r}_{12})\rangle-\langle\boldsymbol{\sigma}_1\cdot\boldsymbol{\sigma}_2\delta(\mathbf{r}_{12})\rangle -\frac{14}{3}Q-\frac{2}{3\pi}M', \tag{4.3}$$

where Q is the principal part of the logarithmically diverging quantity $\mathbf{r}_{12}^{-3}$ and M' is a part of the Bethe logarithm. These results agree with those given by Sucher.

The various contributions for He-like systems have been summarized by Drake [39], who gives the following α^3 contribution for the ground state:

$$\left(\frac{14}{3}\ln\alpha+\frac{164}{15}\right)\langle\delta(\mathbf{r}_{12})\rangle-\frac{14}{3}Q-\frac{2}{3\pi}M. \tag{4.4}$$

This contains also self-energy (vertex correction) and vacuum-polarization contributions. These have been evaluated by Araki with the following results:

$$\Delta E_{\text{vertex}}=\left[-\frac{8}{3}\left(\frac{5}{6}-\ln 2-2\ln\alpha\right) -\frac{2}{3}\langle\boldsymbol{\sigma}_1\cdot\boldsymbol{\sigma}_2\rangle\right]\langle\delta(\mathbf{r}_{12})\rangle-\frac{2}{3\pi}M'', \tag{4.5}$$

$$\Delta E_{\text{vacpol}}=\frac{4}{15}\langle\delta(\mathbf{r}_{12})\rangle, \tag{4.6}$$

where M'' is a second part of the Bethe logarithm. Adding these quantities to the total two-photon exchange above (4.3) gives ($M'+M''=M$)

$$\left[\frac{134}{15}+\frac{14}{3}\ln\alpha-\frac{2}{3}\langle\boldsymbol{\sigma}_1\cdot\boldsymbol{\sigma}_2\rangle\right]\langle\delta(\mathbf{r}_{12})\rangle-\frac{14}{3}Q-\frac{2}{3\pi}M. \tag{4.7}$$

TABLE VI. Coefficients (in hartree units) for the $(Z\alpha)^3$ contributions for electron-electron interaction in heliumlike ions, evaluated by Sucher [6]. The entries should be multiplied by $\langle\delta(\mathbf{r}_{12})\rangle/Z^3$, which for hydrogenic functions has the value $1/8\pi$. The last column gives the expressions for singlet states with $\langle\sigma_1\cdot\sigma_2\rangle=-3$. We have omitted the $-\frac{8}{3}\ln(Z\alpha)$ term occurring in the no-pair contribution to the Coulomb-Breit interaction and the $2\ln(Z\alpha)$ term occurring in the double-pair contribution to the Breit-Breit interaction. The constant D has to be evaluated numerically and is discussed in Appendix C.

Contribution	Coefficient	Singlet state
Coulomb-Coulomb		
No pair	$-(\frac{\pi}{2}+\frac{5}{3})$	
Single pair	2	
Double pair	$(\frac{\pi}{2}-\frac{5}{3})$	
Total Coulomb-Coulomb	$-\frac{4}{3}$	
Coulomb-Breit		
Unretarded	$-\frac{4}{3}(\frac{\pi}{2}+1)\langle\sigma_1\cdot\sigma_2\rangle$	$4(\frac{\pi}{2}+1)$
No pair	$D+\frac{8}{3}\ln 2-\frac{4}{3}(\frac{\pi}{2}+1+\frac{1}{2}\ln 2)\langle\sigma_1\cdot\sigma_2\rangle$	$D+2\pi+4+\frac{14}{3}\ln 2$
Single pair	$\frac{4}{3}(1+\ln 2)\langle\sigma_1\cdot\sigma_2\rangle$	$-4(1+\ln 2)$
Double pair	$\frac{4}{3}(\frac{\pi}{2}-1-\frac{1}{2}\ln 2)\langle\sigma_1\cdot\sigma_2\rangle$	$-4(\frac{\pi}{2}-1-\frac{1}{2}\ln 2)$
Total Coulomb-Breit	$D+\frac{8}{3}\ln 2-\frac{4}{3}\langle\sigma_1\cdot\sigma_2\rangle$	$D+\frac{8}{3}\ln 2+4$
Breit-Breit		
No pair	$-\frac{3\pi}{4}+1+\frac{1}{2}\ln 2+\frac{1}{3}(-\frac{\pi}{4}+1+\frac{1}{2}\ln 2)\langle\sigma_1\cdot\sigma_2\rangle$	$-\frac{\pi}{2}$
Single pair	$1+3\ln 2+\frac{1}{3}(1-\ln 2)\langle\sigma_1\cdot\sigma_2\rangle$	$4\ln 2$
Double pair	$\frac{3\pi}{4}+1-\frac{25}{6}\ln 2+\frac{1}{3}(\frac{\pi}{4}-1+\frac{1}{2}\ln 2)\langle\sigma_1\cdot\sigma_2\rangle$	$\frac{\pi}{2}+2-\frac{14}{3}\ln 2$
Total Breit-Breit	$3-\frac{2}{3}\ln 2+\frac{1}{3}\langle\sigma_1\cdot\sigma_2\rangle$	$2-\frac{2}{3}\ln 2$
Total		
No pair	$D-\frac{5\pi}{4}+\frac{4}{3}+\frac{1}{2}\ln 2-(\frac{3\pi}{4}+1+\frac{1}{2}\ln 2)\langle\sigma_1\cdot\sigma_2\rangle$	$D+\pi+\frac{7}{3}+\frac{14}{3}\ln 2$
Single pair	$3(1+\ln 2)+(\frac{5}{3}+\ln 2)\langle\sigma_1\cdot\sigma_2\rangle$	-2
Double pair	$\frac{5\pi}{4}-\frac{2}{3}-\frac{25}{6}\ln 2+(\frac{3\pi}{4}-\frac{5}{3}-\frac{1}{2}\ln 2)\langle\sigma_1\cdot\sigma_2\rangle$	$\frac{13}{3}-\pi-\frac{8}{3}\ln 2$
Grand total	$D+\frac{5}{3}+2\ln 2-\langle\sigma_1\cdot\sigma_2\rangle$	$D+\frac{14}{3}+2\ln 2$

With $\langle \boldsymbol{\sigma}_1 \cdot \boldsymbol{\sigma}_2 \rangle = -3$ this agrees with the results of Drake [39].

To leading order in a $1/Z$ expansion, Q and M' can be found to be given by

$$Q = -\left(\ln(2Z) - \frac{4}{3}\right)\langle \delta(\mathbf{r}_{12}) \rangle, \tag{4.8}$$

$$-\frac{2}{3\pi}M' = \left(-\frac{16}{3}\ln Z + D\right)\langle \delta(\mathbf{r}_{12}) \rangle, \tag{4.9}$$

where D is a constant that has to be evaluated numerically. With these expressions the Coulomb-Breit and Breit-Breit contributions become, respectively,

$$\left(D + \frac{8}{3}\ln 2 - \frac{8}{3}\ln(Z\alpha)\right)\langle \delta(\mathbf{r}_{12}) \rangle - \frac{4}{3}\langle \boldsymbol{\sigma}_1 \cdot \boldsymbol{\sigma}_2 \delta(\mathbf{r}_{12}) \rangle,$$
$$\left(3 - \frac{2}{3}\ln 2 + 2\ln(Z\alpha)\right)\langle \delta(\mathbf{r}_{12}) \rangle + \frac{1}{3}\langle \boldsymbol{\sigma}_1 \cdot \boldsymbol{\sigma}_2 \delta(\mathbf{r}_{12}) \rangle, \tag{4.10}$$

which give the total contribution

$$\left(D + \frac{5}{3} + 2\ln 2 - \frac{2}{3}\ln(Z\alpha)\right)\langle \delta(\mathbf{r}_{12}) \rangle - \langle \boldsymbol{\sigma}_1 \cdot \boldsymbol{\sigma}_2 \delta(\mathbf{r}_{12}) \rangle. \tag{4.11}$$

We have evaluated the constant D to be -1.9091 (see Appendix C), which is in reasonable agreement with the value -1.88 obtained by Blundell *et al.* [9]. Our value is expected to be accurate to the digits given.

In Fig. 2 we have displayed the Coulomb-Coulomb, Coulomb-Breit, and total contributions after dividing by $(Z\alpha)^2$. The slope at the origin represents the coefficient of the $(Z\alpha)^3$ term. In Fig. 3 the corresponding results are

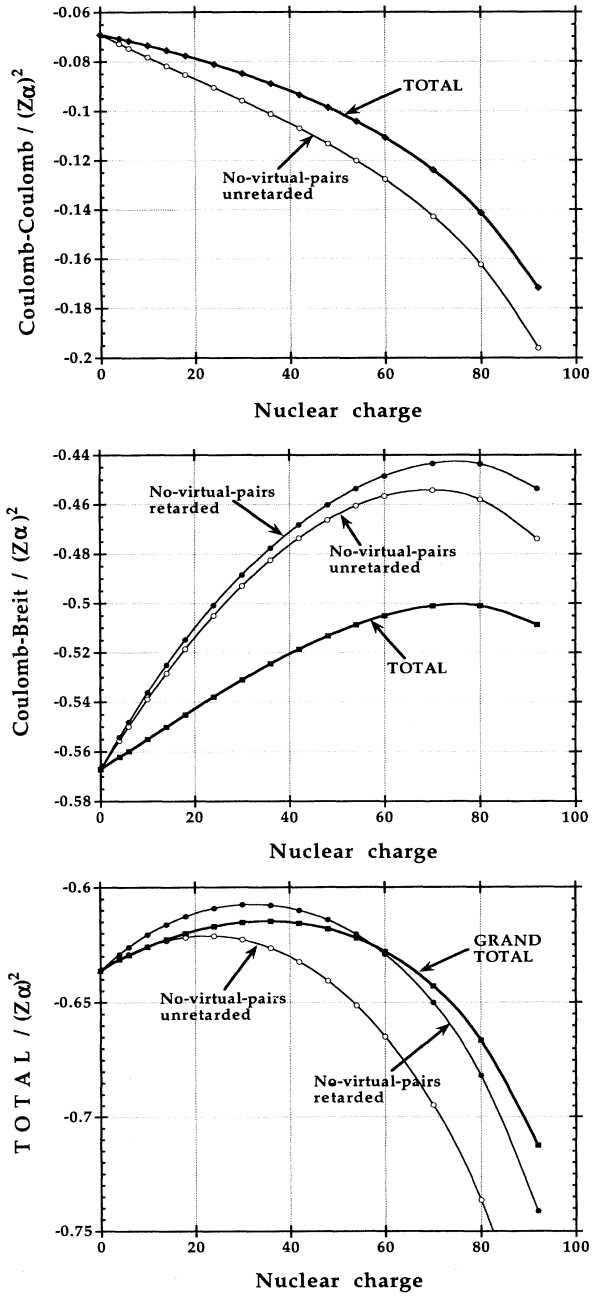

FIG. 2. Contributions to the two-photon exchange divided by $(Z\alpha)^2$ after subtracting the zeroth-order and the $(Z\alpha)^3\ln(Z\alpha)$ terms. The slope at the origin represents the $(Z\alpha)^3$ coefficient.

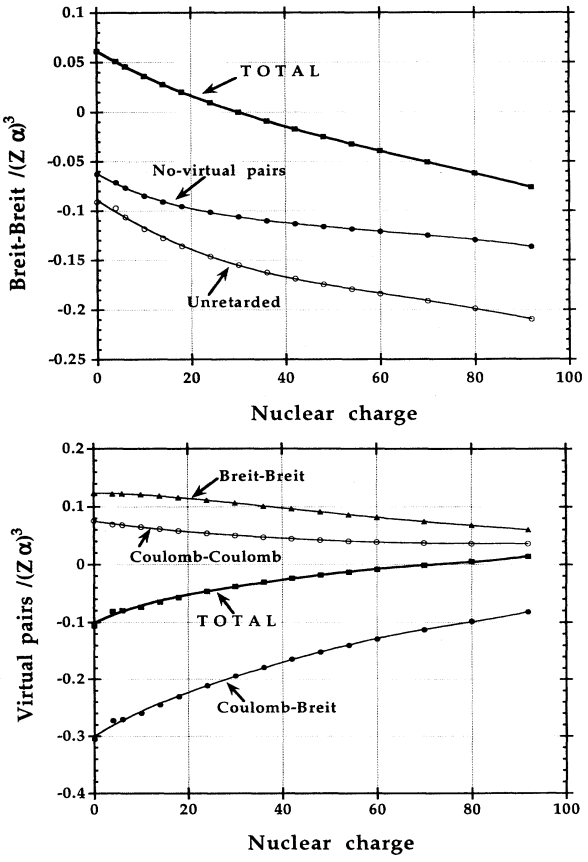

FIG. 3. Contributions to the two-photon exchange due to the Breit-Breit interaction and to virtual pairs after dividing by $(Z\alpha)^3$. The points at the origin represent the analytical values of Sucher.

shown for the Breit-Breit contribution as well as for that of the virtual pairs after dividing by $(Z\alpha)^3$. The value at the origin is the analytical coefficient of the $(Z\alpha)^3$ term.

In order to compare our numerical results with the analytical results, we have made fits to a $(Z\alpha)^n$ expansion by a least-squares procedure after subtracting off the $(Z\alpha)^3 \ln(Z\alpha)$ terms. The zeroth-order nonrelativistic value $-157\,666.43$ hartree, which is known with high accuracy, has been used. The second-order terms $(Z\alpha)^2$, on the other hand, do not seem to be known with sufficient accuracy and have been used as adjustable parameters.

The $(Z\alpha)^3$ and $(Z\alpha)^4$ coefficients obtained in the fit are given in Table VII. The parameters obtained in the fit agree well with the theoretical predictions of Sucher (using $D = -1.9091$), in most cases within a few percent. We have also tried to fit the data to a $(Z\alpha)^n$ expansion with a $(Z\alpha)^4 \ln(Z\alpha)$ term, but this was not stable enough to yield any sensible results.

In Fig. 4 we have plotted the one- and two-photon contributions, divided by the single-electron energy. The vertical scale is logarithmic, so that -1 corresponds to α, -2 to α^2, etc. It can then be seen that the Coulomb (one-photon) and Coulomb-Coulomb contributions start at $\alpha^0 = 1$ for low Z, while the Breit (one-photon) and Coulomb-Breit contributions start at α^2. The next-order effects, Breit-Breit contributions, and QED effects (retardation and virtual pairs) start at α^3. In the high-Z region it can be seen that the single-photon contributions tend toward α, while *all* two-photon contributions tend towards α^2.

It can be seen from the figure that the QED effect is quite comparable to the Breit-Breit contribution. This is displayed in more detail in Fig. 5, where we show the contributions from retardation and virtual pairs and the reference state separately. The effects of retardation and virtual pairs have opposite signs and largely cancel each other for low Z.

In Fig. 6 we have, in addition, displayed the separate contributions from single and double pairs and in Fig. 7 the contributions from crossed photons. In the latter figure we have also indicated the corresponding effect in the Feynman gauge in a few cases. This demonstrates clearly, as emphasized previously, the large difference between the two gauges for low Z. For high Z, on the other hand, the contributions from crossed photons tend to the same limit in the two gauges.

TABLE VII. Coefficients for $(Z\alpha)^n$ from the least-squares fit of the numerical data. The $(Z\alpha)^3$ coefficients are compared with theoretical predictions of Sucher [6] using $D = -1.9091$. The term "unretarded" represents results without retardation and without virtual pairs (negative-energy states); "no virtual pairs" represents results with retardation, but without virtual pairs (in hartree units).

Contribution	$(Z\alpha)^2$	$(Z\alpha)^3$ Numerical	$(Z\alpha)^3$ Sucher	$(Z\alpha)^4$ Numerical
Coulomb-Coulomb	-0.0692(2)			
Unretarded=NVP		-0.129(2)	-0.12881	0.07(2)
Virtual pairs		0.075(2)	0.07576	-0.16(2)
Total		-0.054(2)	-0.05305	-0.09(2)
Coulomb-Breit	-0.5670(2)			
Unretarded		0.410(3)	0.40915	-0.27(3)
No virtual pairs		0.460(4)	0.46190	-0.52(2)
Virtual pairs		-0.300(5)	-0.30516	0.66(4)
Total		0.159(4)	0.15674	0.14(2)
QED=total−unretarded		-0.250(3)	-0.25242	0.41(2)
Breit-Breit	0			
Unretarded		-0.093(3)	-0.09085[a]	-0.43(3)
No virtual pairs		-0.070(5)	-0.06250	-0.34(4)
Virtual pairs		0.128(3)	0.12369	-0.03(3)
Total		0.058(3)	0.06119	-0.37(3)
QED=total−unretarded		0.151(3)	0.15204	0.06(1)
Total	-0.6362(3)			
Unretarded		0.186(5)	0.18950[b]	-0.64(3)
No virtual pairs		0.260(6)	0.27058	-0.78(8)
Virtual pairs		-0.099(5)	-0.10570	0.46(5)
Grand total	-0.6362(3)	0.162(3)	0.16488	-0.32(3)
QED=total−unretarded	0	-0.023(3)	-0.02462	0.31(3)

[a]This value is deduced from the other unretarded values in this column.
[b]This value is taken from Ref. [9].

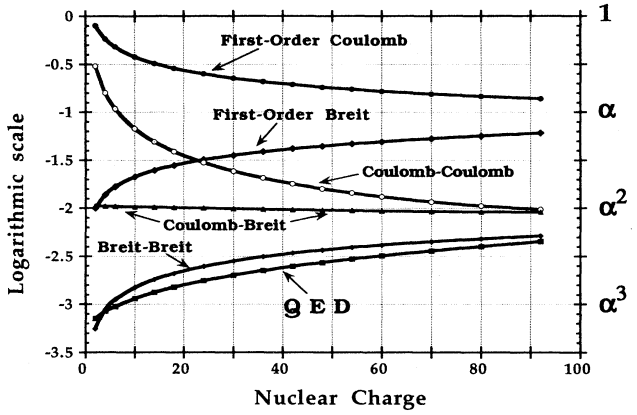

FIG. 4. Contributions due to one- and two-photon exchange divided by the one-electron energy. The vertical scale is logarithmic, so that 0 corresponds to unity, -1 to α, -2 to α^2, etc.

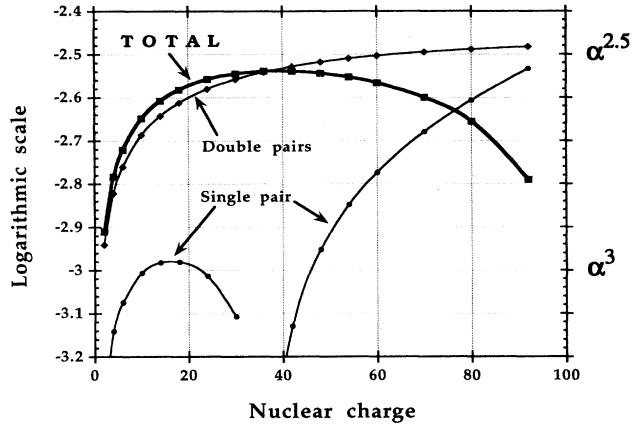

FIG. 6. Same plot as in Fig. 4, but for the virtual-pair effects from Fig. 5 separated into effects of single and double virtual pairs.

V. CONCLUSIONS

Several important general conclusions can be drawn from the analysis presented here. As mentioned in the Introduction, the Breit interaction becomes quite important for highly charged ions, also for moderately high Z. For the heliumlike systems studied here, the first-order Breit interaction dominates over the electron correlation (Coulomb-Coulomb) already at $Z = 25$. The iterated Breit interaction (Breit-Breit), on the other hand, is about two orders of magnitude smaller and of the same order as the retardation and virtual-pair effects.

The iterated Breit interaction is also considerably smaller than the effect of a single Breit interaction, combined with one or several Coulomb interactions (Coulomb-Breit) at least for low and medium-high Z. Therefore, the *standard no-virtual-pair approximation* (NVPA), where one Breit interaction is included together with the iterated Coulomb interaction, neglecting retardation and virtual-pair effects, is quite a good approximation for such systems. The same can be expected to be true for heavy ions that are moderately highly charged, i.e., with a medium-high effective nuclear charge for the outer electrons.

Several attempts have been made to include the retardation of the Breit interaction in an approximate way by means of a modified potential. The present analysis indicates strongly, however, that such a procedure is not meaningful, unless also virtual-pair effects are considered.

In order to go beyond the standard NVPA, discussed above, it is, according to the present analysis, necessary to include retardation *and* virtual-pair effects together with the iterated Breit interaction. To include only the latter, leaving out the QED effects (retardation and virtual pairs), would not represent any major improvement over the simpler standard NVPA.

It should be emphasized again that radiative effects (Lamb shifts) are not considered in this work. The single-electron Lamb shift is, for high Z, of the same order

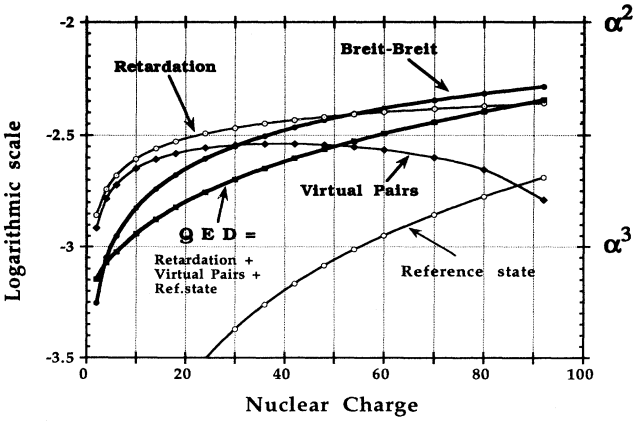

FIG. 5. Same plot as in Fig. 4, but for the QED effects separated into effects of retardation, virtual pairs, and reference state. For comparison the unretarded Breit-Breit effect is also included.

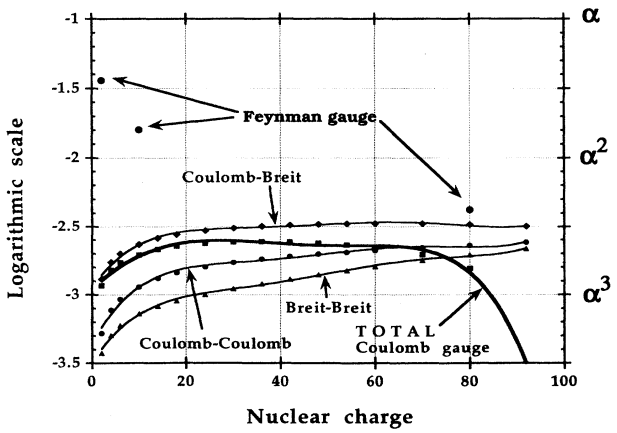

FIG. 7. Same plot as in Fig. 4, but for the part of the QED effects coming from crossed photons. The contribution from the reference state is not included.

as the single-photon contributions. This shift is known with high accuracy [40] and can easily be added to the energy level. The two-body Lamb shift (screening effect) is comparable to the QED effects considered here and consequently also has to be taken into account in going beyond the standard NVPA in a sensible way.

ACKNOWLEDGMENTS

Financial support was provided by the Swedish Natural Research Council (NFR) and the Knut and Alice Wallenberg Foundation. The authors wish to acknowledge stimulating discussions with Joe Sucher, Steve Blundell, Ann-Marie Mårtensson-Pendrill, Eva Lindroth, Håkan Warston, and Per Sunnergren. Walter Johnson and Jonathan Sapirstein are gratefully acknowledged for allowing us to use their unpublished RMBPT results.

APPENDIX A: THE REFERENCE-STATE CONTRIBUTION

Consider the two-photon electron exchange contributions given by the energy shift formula in Eq. (2.1). The degenerate states, both for the uncrossed and the crossed diagram, and the squared second-order counterterm give rise to a finite contribution. This contribution, which is gauge independent, is derived in this section. For simplicity we shall use the Feynman gauge when writing down the expressions.

The ladder contribution to the energy shift is given by Eq. (2.2). We restrict the discussion to the reference-state contribution from the ground state of He-like atoms, i.e., $e_0 = e_a = e_b = e_c = e_d$. For simplicity we define a function

$$g_{dcba}(z) = \int d^3\mathbf{x}_1 \int d^3\mathbf{x}_2 \frac{-c}{\epsilon_0} \int \frac{d^3\mathbf{k}}{(2\pi)^3} \frac{e^{i\mathbf{k}\cdot(\mathbf{x}_2-\mathbf{x}_1)}}{(z^2 - c^2\mathbf{k}^2 + i\epsilon)} \times \Phi_d^\dagger(\mathbf{x}_2)\alpha_\mu\Phi_c(\mathbf{x}_2)\Phi_b^\dagger(\mathbf{x}_1)\alpha^\mu\Phi_a(\mathbf{x}_1), \tag{A1}$$

where the functions Φ_a, Φ_b, Φ_c, and Φ_d may differ in the spin part. The angular integrations, considered in Appendix B, give further restrictions on the spin directions. We use the subscript lad to indicate the angular characteristic of the ladder diagram, which shall be distinguished from the angular characteristic of the crossed ladder diagram. Adopting this notation, we can write the ladder contribution as

$$\begin{aligned}\langle\Phi_a^0 \mid S^4_{\mathrm{lad},\gamma} \mid \Phi_a^0\rangle = c^2e^4 &\int_{-\infty}^{\infty}\frac{dz_1}{2\pi}\int_{-\infty}^{\infty}\frac{dz_2}{2\pi}\int_{-\infty}^{\infty}\frac{dz_3}{2\pi}\int_{-\infty}^{\infty}\frac{dz_4}{2\pi} \\ &\times \frac{1}{[z_3 - e_0(1-i\eta)]}\frac{1}{[z_4 - e_0(1-i\eta)]}\sum_{\mathrm{lad}} g_{d'c'b'a'}(z_2)g_{dcba}(z_1) \\ &\times \int_{-\infty}^{\infty} dt_4 e^{-i(z_4+z_2-e_0)t_4}e^{-\gamma|t_4|}\int_{-\infty}^{\infty} dt_3 e^{-i(z_3-z_2-e_0)t_3}e^{-\gamma|t_3|} \\ &\times \int_{-\infty}^{\infty} dt_2 e^{-i(z_1-z_4+e_0)t_2}e^{-\gamma|t_2|}\int_{-\infty}^{\infty} dt_1 e^{-i(e_0-z_3-z_1)t_1}e^{-\gamma|t_1|}.\end{aligned} \tag{A2}$$

We now introduce a Δ_γ function defined by

$$\Delta_\gamma(x) = \int_{-\infty}^{\infty}\frac{dt}{2\pi}e^{-ixt}e^{-\gamma|t|} = \frac{1}{\pi}\frac{\gamma}{x^2+\gamma^2}, \tag{A3}$$

which has the properties

$$\lim_{\gamma\to 0}\Delta_\gamma(x) = \delta(x), \tag{A4}$$

$$\lim_{\gamma\to 0}\pi\gamma\Delta_\gamma(x) = \delta_{x,0}. \tag{A5}$$

Thus the ladder part can be expressed as

$$\begin{aligned}\langle\Phi_a^0 \mid S^4_{\mathrm{lad},\gamma} \mid \Phi_a^0\rangle = \frac{c^2e^4}{\pi^4}&\int_{-\infty}^{\infty}dz_1\int_{-\infty}^{\infty}dz_2\int_{-\infty}^{\infty}dz_3\int_{-\infty}^{\infty}dz_4 \frac{1}{[z_3 - e_0(1-i\eta)]}\frac{1}{[z_4 - e_0(1-i\eta)]}\sum_{\mathrm{lad}} g_{d'c'b'a'}(z_2)g_{dcba}(z_1) \\ &\times \frac{\gamma}{(e_0-z_4-z_2)^2+\gamma^2}\frac{\gamma}{(e_0-z_4+z_1)^2+\gamma^2}\frac{\gamma}{(e_0-z_3-z_1)^2+\gamma^2}\frac{\gamma}{(e_0-z_3+z_2)^2+\gamma^2}.\end{aligned} \tag{A6}$$

By using the integral identity

$$\begin{aligned}f_\gamma(z_2,z_1) &= \int_{-\infty}^{\infty}dz\frac{1}{[z-e_0(1-i\eta)]}\frac{\gamma}{(e_0-z-z_2)^2+\gamma^2}\frac{\gamma}{(e_0-z+z_1)^2+\gamma^2} \\ &= \frac{\pi\gamma}{(z_2+z_1)^2+4\gamma^2}\frac{(z_2-z_1-4i\gamma)}{(z_2-i\gamma)(z_1+i\gamma)}\end{aligned} \tag{A7}$$

we can perform the z_3 and z_4 integrations, yielding the expression

$$\langle\Phi_a^0 \mid S_{\mathrm{lad},\gamma}^4 \mid \Phi_a^0\rangle = \frac{c^2e^4}{\pi^4}\int dz_1 \int dz_2 f_\gamma(z_2,z_1) f_\gamma(z_1,z_2) \sum_{\mathrm{lad}} g_{d'c'b'a'}(z_2) g_{dcba}(z_1). \tag{A8}$$

In a similar way we can obtain the crossed ladder contribution

$$\begin{aligned}\langle\Phi_a^0 \mid S_{\mathrm{cro},\gamma}^4 \mid \Phi_a^0\rangle &= \frac{c^2e^4}{\pi^4}\int_{-\infty}^{\infty} dz_1 \int_{-\infty}^{\infty} dz_2 \int_{-\infty}^{\infty} dz_3 \int_{-\infty}^{\infty} dz_4 \\ &\times \frac{1}{[z_3 - e_0(1-i\eta)]}\frac{1}{[z_4 - e_0(1-i\eta)]}\sum_{\mathrm{cro}} g_{d'c'b'a'}(z_2) g_{dcba}(z_1) \\ &\times \frac{\gamma}{(e_0 - z_4 + z_2)^2+\gamma^2}\frac{\gamma}{(e_0 - z_4 - z_1)^2+\gamma^2}\frac{\gamma}{(e_0 - z_3 - z_1)^2+\gamma^2}\frac{\gamma}{(e_0 - z_3 + z_2)^2+\gamma^2} \\ &= \frac{c^2e^4}{\pi^4}\int dz_1 \int dz_2 f_\gamma(z_2,z_1) f_\gamma(z_2,z_1) \sum_{\mathrm{cro}} g_{d'c'b'a'}(z_2) g_{dcba}(z_1),\end{aligned} \tag{A9}$$

where the subscript cro indicates the angular characteristic of the crossed ladder contribution.

In order to handle the divergent part of the ladder diagram, we focus on the squared one-photon counterpart, which has to be subtracted in order to obtain the finite ladder contribution. Following standard rules, we can write the one-photon counterpart as

$$\langle\Phi_a^0 \mid S_{\mathrm{red},\gamma}^2 \mid \Phi_a^0\rangle = -i\frac{ce^2}{2\pi}\int_{-\infty}^{\infty} dz \frac{4\gamma^2}{(z^2+\gamma^2)^2} g_{dcba}(z). \tag{A10}$$

Consider the sum

$$f_\gamma(z_2,z_1) + f_\gamma(z_1,z_2) = \frac{\pi\gamma}{(z_2+z_1)^2+4\gamma^2}\left\{\frac{(z_2 - z_1 - 4i\gamma)}{(z_2 - i\gamma)(z_1 + i\gamma)} + \frac{(z_1 - z_2 - 4i\gamma)}{(z_1 - i\gamma)(z_2 + i\gamma)}\right\} = -\frac{2\pi\gamma^2 i}{(z_1^2+\gamma^2)(z_2^2+\gamma^2)} \tag{A11}$$

and the square of the sum

$$\frac{1}{2}[f_\gamma(z_2,z_1) + f_\gamma(z_1,z_2)]^2 = \frac{-2\pi^2\gamma^4}{(z_1^2+\gamma^2)^2(z_2^2+\gamma^2)^2}. \tag{A12}$$

By using the above identity we can rewrite the squared one-photon counterpart as

$$\begin{aligned}\langle\Phi_a^0 \mid S_{\mathrm{red},\gamma}^2 \mid \Phi_a^0\rangle^2 &= \frac{-c^2e^4}{4\pi^2}\int_{-\infty}^{\infty} dz_1 \int_{-\infty}^{\infty} dz_2 \frac{4\gamma^2}{(z_2^2+\gamma^2)^2}\frac{4\gamma^2}{(z_1^2+\gamma^2)^2}\sum_{\mathrm{lad}} g_{d'c'b'a'}(z_2) g_{dcba}(z_1) \\ &= \frac{c^2e^4}{\pi^4}\int_{-\infty}^{\infty} dz_1 \int_{-\infty}^{\infty} dz_2 [f_\gamma(z_2,z_1) + f_\gamma(z_1,z_2)]^2 \sum_{\mathrm{lad}} g_{d'c'b'a'}(z_2) g_{dcba}(z_1)\end{aligned} \tag{A13}$$

and since the ladder contribution is given by

$$\begin{aligned}\langle\Phi_a^0 \mid S_{\mathrm{lad},\gamma}^4 \mid \Phi_a^0\rangle &= \frac{c^2e^4}{\pi^4}\int dz_1 \int dz_2 f_\gamma(z_2,z_1) f_\gamma(z_1,z_2) \sum_{\mathrm{lad}} g_{d'c'b'a'}(z_2) g_{dcba}(z_1) \\ &= \frac{c^2e^4}{\pi^4}\int dz_1 \int dz_2 \left\{\frac{1}{2}[f_\gamma(z_2,z_1) + f_\gamma(z_1,z_2)]^2 \right. \\ &\left. -\frac{1}{2}[f_\gamma^2(z_2,z_1) + f_\gamma^2(z_1,z_2)]\right\} \sum_{\mathrm{lad}} g_{d'c'b'a'}(z_2) g_{dcba}(z_1),\end{aligned} \tag{A14}$$

we can directly subtract the squared one-photon counterterm from it to obtain

$$(4\langle\Phi_a^0 \mid S_{\mathrm{lad},\gamma}^4 \mid \Phi_a^0\rangle - 2\langle\Phi_a^0 \mid S_{\mathrm{red},\gamma}^2 \mid \Phi_a^0\rangle^2) = \frac{-c^2e^4}{\pi^4}\int dz_1 \int dz_2 2[f_\gamma^2(z_2,z_1) + f_\gamma^2(z_1,z_2)] \sum_{\mathrm{lad}} g_{d'c'b'a'}(z_2) g_{dcba}(z_1). \tag{A15}$$

Thus we can write the finite reference-state contribution from two-photon exchange as

$$\Delta E_A^{4,\mathrm{ref}} = \lim_{\gamma\to 0}\frac{1}{2}i\gamma\{(4\langle\Phi_a^0 \mid S^4_{\mathrm{lad},\gamma} \mid \Phi_a^0\rangle + 4\langle\Phi_a^0 \mid S^4_{\mathrm{cro},\gamma} \mid \Phi_a^0\rangle - 2\langle\Phi_a^0 \mid S^2_{\mathrm{red},\gamma} \mid \Phi_a^0\rangle^2)\}$$
$$= \lim_{\gamma\to 0}\frac{1}{2}i\gamma\frac{-c^2e^4}{\pi^4}\int dz_1\int dz_2\Bigg\{2[f_\gamma^2(z_2,z_1)+f_\gamma^2(z_1,z_2)]\sum_{\mathrm{lad}} g_{d'c'b'a'}(z_2)g_{dcba}(z_1)$$
$$-4f_\gamma^2(z_2,z_1)\sum_{\mathrm{cro}} g_{d'c'b'a'}(z_2)g_{dcba}(z_1)\Bigg\} \tag{A16}$$

or, since

$$f_\gamma(-z_2,-z_1) = f_\gamma(z_1,z_2) \tag{A17}$$

and

$$g_{dcba}(z) = g_{dcba}(-z), \tag{A18}$$

we can rewrite Eq. (A16) as

$$\Delta E_A^{4,\mathrm{ref}} = \lim_{\gamma\to 0}\frac{1}{2}i\gamma\frac{-e^4}{\pi^4}\int dz_1\int dz_2\left\{4f_\gamma^2(z_2,z_1)\sum_{\mathrm{lad}} g_{d'c'b'a'}(z_2)g_{dcba}(z_1) - 4f_\gamma^2(z_2,z_1)\sum_{\mathrm{cro}} g_{d'c'b'a'}(z_2)g_{dcba}(z_1)\right\}. \tag{A19}$$

Apart from the sign, the only thing that differs between the finite ladder and the crossed ladder contribution is the angular structure of the diagrams. Thus, since the angular part of the respective diagrams differs only for the vector-vector ($\nu,\mu = 1-3$) interaction, there will only be finite remainder from the vector-vector part.

To obtain an expression that is appropriate for numerical calculations we also perform the z_2 integration analytically. By extracting the z_2- and z_1-dependent parts out of g_{dcba} we can use residue calculus in the lower half plane, with poles at $z_2 = \sqrt{c^2k_2^2 - i\epsilon}$ and $z_2 = -z_1 - 2i\gamma$, to obtain

$$\int dz_2 i\gamma\, f_\gamma^2(z_2,z_1)\frac{1}{(z_2^2 - c^2\mathbf{k}_2^2 + i\epsilon')(z_1^2 - c^2\mathbf{k}_1^2 + i\epsilon)}$$
$$= \int dz_2 \frac{\pi^2\gamma^2(z_2 - z_1 - 4i\gamma)^2}{[(z_2+z_1)^2+4\gamma^2]^2(z_2 - i\gamma)^2(z_1+i\gamma)^2}\frac{1}{(z_2^2 - c^2\mathbf{k}_2^2 + i\epsilon')(z_1^2 - c^2\mathbf{k}_1^2 + i\epsilon)}$$
$$= \frac{\pi^3}{4}\Bigg\{\frac{(-44i\gamma^3 - 5i\gamma c^2k_2^2 - 44\gamma^2 z_1 - ck_2z_1 + 13i\gamma z_1^2 + z_1^3)}{(3i\gamma+z_1)(4\gamma^2 + c^2k_2^2 - 4i\gamma z_1 - z_1^2)^2(z_1+i\gamma)^2}$$
$$- \frac{\gamma^3(-4i\gamma + ck_2 - z_1)^2}{ck_2(i\gamma + c^2k_2)^2[4\gamma^2 + (ck_2+z_1)^2]^2(z_1+i\gamma)^2}\Bigg\}\frac{1}{(z_1^2 - c^2\mathbf{k}_1^2 + i\epsilon)}. \tag{A20}$$

In a similar way we perform the z_1 integration, with poles at $z_1 = -\sqrt{c^2k_2^2 - i\epsilon}$ and $z_1 = -ck_2 + 2i\gamma$, and finally we take the limit $\gamma\to 0$, which yields

$$\lim_{\gamma\to 0}\frac{-ic^2e^4}{2\pi^4}\int dz_2\int dz_1 4f_\gamma^2(z_2,z_1)$$
$$\times\frac{1}{(z_2^2 - c^2\mathbf{k}_2^2 + i\epsilon')(z_1^2 - c^2\mathbf{k}_1^2 + i\epsilon)}$$
$$= \frac{e^4}{2c^2}\frac{(k_1^2 + k_1k_2 + k_2^2)}{k_1^3k_2^3(k_1+k_2)}. \tag{A21}$$

The reference-state contribution for the crossed ladder diagram can also be obtained by letting $q, q'\to 0$ in Eq. (2.26), since the singular reference part appears only in the ladder diagram. Since the ladder and crossed ladder contributions only differ by simple angular factors, the total reference-state contribution can thus also easily be achieved from the crossed ladder part.

APPENDIX B: EVALUATION OF THE ANGULAR FACTORS FOR TWO-PHOTON EXCHANGE

We want to evaluate the angular part of the two-photon Feynman diagrams given in Fig. 1. As a first step we evaluate the angular part of the first interaction at the bottom of the ladder diagram in Fig. 1(a), which has the mathematical expression

$$(2L+1)\langle t \mid \alpha^\mu j_L(kr)\mathbf{C}^L \mid a\rangle\cdot\langle t \mid \alpha_\mu j_L(kr)\mathbf{C}^L \mid b\rangle. \tag{B1}$$

Using angular-momentum graphs the angular part can be expressed as

$$(-1)^{L+S}(2L+1)\langle l_t \parallel \mathbf{C}^L \parallel l_a\rangle\cdot\langle l_u \parallel \mathbf{C}^L \parallel l_b\rangle$$
$$\times\langle \tfrac{1}{2} \parallel \boldsymbol{\sigma}+^S \parallel \tfrac{1}{2}\rangle^2 \times \mathrm{A1}, \tag{B2}$$

where A1 is the angular-momentum graph shown in Fig. 8. Here $S = 0$ for the scalar part and $S = 1$ for the vector part of $\alpha_1^\mu \alpha_{\mu 2} = 1 - \boldsymbol{\alpha}_1 \cdot \boldsymbol{\alpha}_2$. The minus sign of the alpha part is included in the integral and not in the angular factor. The ls convention is employed. The square of the reduced matrix element of the spin part is

$$\langle \tfrac{1}{2} \parallel \boldsymbol{\sigma}^S \parallel \tfrac{1}{2} \rangle^2 = 2(2S+1). \tag{B3}$$

The graph A1 in Fig. 8 can be transformed into the graph A2 in Fig. 9 with a summation over κ and κ' and the expression in Eq. (B2) can be rewritten as

$$\sum_{\kappa\kappa'} (-1)^{L+S+l_a+l_b+\kappa+\kappa'+1} 2(2S+1)(2L+1) \times [\kappa,\kappa',j_a,j_b]^{\frac{1}{2}} \begin{Bmatrix} \kappa & S & j_a \\ \frac{1}{2} & l_a & \frac{1}{2} \end{Bmatrix} \begin{Bmatrix} \kappa' & S & j_b \\ \frac{1}{2} & l_b & \frac{1}{2} \end{Bmatrix} \times \langle j_t \parallel \mathbf{C}^L \parallel j_\kappa \rangle \cdot \langle j_u \parallel \mathbf{C}^L \parallel j_{\kappa'} \rangle \times \text{A3}, \tag{B4}$$

where A3 is the angular-momentum graph shown in Fig. 10(a) and $[\kappa,\kappa',\ldots] = (2\kappa+1)(2\kappa'+1)\cdots$. The reduced matrix element in the jm scheme is given by

$$\langle j_b \parallel \mathbf{C}^L \parallel j_a \rangle = (-1)^{j_b+\frac{1}{2}} [j_a,j_b]^{\frac{1}{2}} \begin{pmatrix} j_b & L & j_a \\ \frac{1}{2} & 0 & -\frac{1}{2} \end{pmatrix}, \tag{B5}$$

provided l_a, L, and l_b satisfy the triangular and parity conditions.

The angular factor associated with the radial integral with large components of states a and b is denoted by AFF, the angular factor associated with the large component of a and the small component of b is denoted by AFG, etc. Therefore, in AFG l_b is, in Eq. (B4), replaced by $\bar{l}_b = 2j_b - l_b$, in AGF, l_a is replaced by $\bar{l}_a = 2j_a - l_a$, and in AGG both these replacements are made. Since the radial part of the small component is purely imaginary, there is a sign change when the small component appears in the bra state. This is compensated for by keeping l_a and l_b in the phase factor.

The graph in Fig. 10(a) can be reduced by coupling the momenta L and S to a resulting momentum K giving

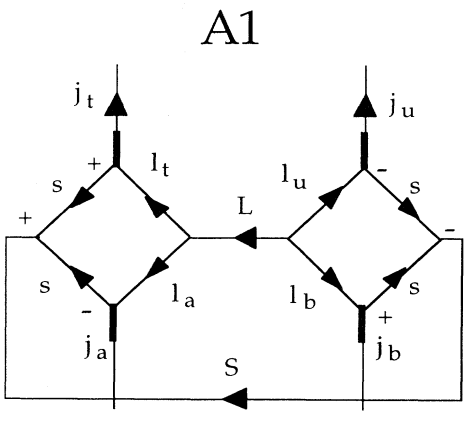

FIG. 8. Angular momentum graph corresponding to a one-photon exchange. L is the tensor rank of the interaction in the orbital space and S the tensor rank in the spin space.

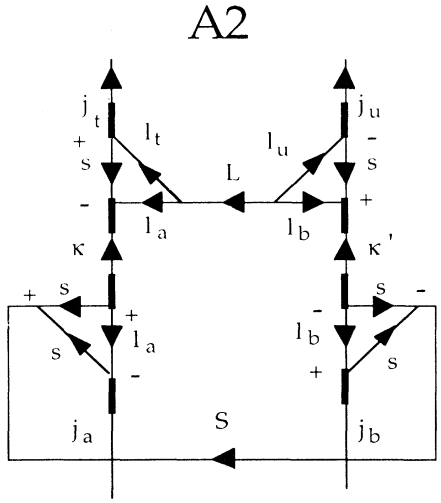

FIG. 9. Same angular momentum graph as in Fig. 8, but with the spin of the outgoing electron coupled with the orbital angular momentum of the incoming electron to κ and κ', respectively, in the two vertices.

$$\sum_K (2K+1) \begin{Bmatrix} j_t & K & j_a \\ S & \kappa & L \end{Bmatrix} \begin{Bmatrix} j_u & K & j_b \\ S & \kappa' & L \end{Bmatrix} \times \text{A4}, \tag{B6}$$

where A4 is the angular-momentum graph in Fig. 10(b). The final reduction of the angular factor in Eq. (B2) then becomes

$$\sum_{k,k'} (-1)^{L+S+l_a+l_b+\kappa+\kappa'+1} 2(2S+1)(2L+1) \times [\kappa,\kappa',j_a,j_b]^{\frac{1}{2}} \begin{Bmatrix} \kappa & S & j_a \\ \frac{1}{2} & l_a & \frac{1}{2} \end{Bmatrix} \begin{Bmatrix} \kappa' & S & j_b \\ \frac{1}{2} & l_b & \frac{1}{2} \end{Bmatrix} \times \langle j_t \parallel \mathbf{C}^L \parallel j_\kappa \rangle \cdot \langle j_u \parallel \mathbf{C}^L \parallel j_{\kappa'} \rangle \sum_K (2K+1) \times \begin{Bmatrix} j_t & K & j_a \\ S & \kappa & L \end{Bmatrix} \begin{Bmatrix} j_u & K & j_b \\ S & \kappa' & L \end{Bmatrix} \times \text{A4}. \tag{B7}$$

In a similar way we get the angular factors for the second interaction at the top of the ladder diagram in Fig. 1(a), which has the mathematical expression

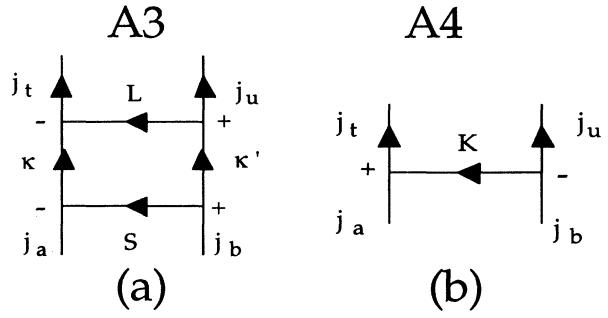

FIG. 10. (a) Angular momentum graph from the reduction of the graph in Fig. 9. (b) Angular momentum graph resulting from further reduction of the graph in (a) when the orbital and spin ranks of the interaction have been coupled to K.

$$(2L+1)\langle c \mid \alpha^\mu j_L(kr)\mathbf{C}^L \mid t\rangle \cdot \langle d \mid \alpha_\mu j_L(kr)\mathbf{C}^L \mid u\rangle \tag{B8}$$

by making the replacements $a \to t$, $t \to c = a$ and $b \to u$, $u \to d = b$. Since the angular factor AFF is associated with the radial integral with the large components of the states a and b, etc., l_a and l_b in the formula [Eq. (B4)] are replaced by $\bar{l}_t$ and $\bar{l}_u$, respectively. In the phase factor l_t and l_u should appear for the same reason as before.

The angular-momentum graph corresponding to the Feynman ladder diagram is given in Fig. 11(a). The reduction of this graph gives

$$(-1)^{j_a+j_d+j_t+j_u+K+K'} \begin{Bmatrix} j_t & J & j_u \\ J_d & K' & j_c \end{Bmatrix} \begin{Bmatrix} j_t & J & j_u \\ j_b & K & j_a \end{Bmatrix}. \tag{B9}$$

For $J = 0$ this reduces to

$$[j_t \cdot j_u, j_a, j_b]^{-\frac{1}{2}} \delta(j_a, j_b)\delta(j_t, j_u)\delta(j_c, j_d) = [j_t, j_a]^{-1}. \tag{B10}$$

For the crossed photon diagram in Fig. 1(b) we evaluate the two one-photon interactions

$$(2L+1)\langle t \mid \alpha^\mu j_L(kr)\mathbf{C}^L \mid a\rangle \cdot \langle d \mid \alpha_\mu j_L(kr)\mathbf{C}^L \mid u\rangle \tag{B11}$$

and

$$(2L+1)\langle c \mid \alpha^\mu j_L(kr)\mathbf{C}^L \mid t\rangle \cdot \langle u \mid \alpha_\mu j_L(kr)\mathbf{C}^L \mid b\rangle \tag{B12}$$

by similar replacements as for the ladder diagram. The angular-momentum graph corresponding to the crossed photon Feynman diagram is given in Fig. 11(b). The reduction of this graph gives

$$(-1)^{j_b+j_c+K+K'+J} \begin{Bmatrix} K & j_u & j_d \\ j_t & K' & j_c \\ j_a & j_b & J \end{Bmatrix}. \tag{B13}$$

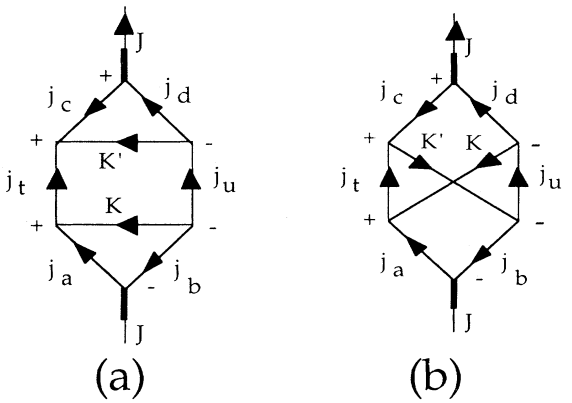

FIG. 11. Angular momentum graphs corresponding to the (a) ladder and (b) crossed two-photon exchange diagrams where the orbital and spin ranks of the interactions have been coupled to K and K', respectively.

For $J = 0$ this reduces to

$$(-1)^{j_t+j_u+K+K'} \begin{Bmatrix} j_t & K' & j_c \\ j_u & K & j_a \end{Bmatrix} [j_c \cdot j_a]^{-\frac{1}{2}} \delta(j_a, j_b)\delta(j_c, j_d). \tag{B14}$$

APPENDIX C: EVALUATION OF THE BETHE LOGARITHM

The expression for M' in Eq. (4.3) is given by Araki [30] and Sucher [6] as

$$M' = \left\langle \Psi \left| \mathbf{p}_1 (H-E) \ln\left(\frac{H-E}{A}\right) \mathbf{p}_2 \right| \Psi \right\rangle + \mathbf{p}_1 \leftrightarrow \mathbf{p}_2, \tag{C1}$$

where $\Psi = \Psi_0 + \Psi_1 + \cdots$ is the nonrelativistic two-electron wave function that is an eigenfunction with the eigenvalue $E = E_0 + E_1 + \cdots$ of the Schrödinger Hamiltonian $H = H_0 + V$, where $V = 1/r_{12}$. In Sucher's treatment this term comes from one transverse photon exchange including an arbitrary number of NVP Coulomb ladder interactions. It corresponds to the retardation effects for the low photon energies up to a cutoff A, where the electron excitation energies are neglected compared to A. The dependence on A cancels when combined with the corresponding contributions from photon energies larger than A. For simplicity A is set to 1 a.u. in the definition of M', although the average electron excitation energy is much larger. Effectively, M' thus has contributions from both low and medium photon energies. Usually M' is combined with a similar expression M'', which is diagonal in the $\mathbf{p}_i$ operators, to form the full Bethe logarithm M. M'' originates from the self-energy diagram with Coulomb-ladder interactions on the internal (vertex corrections) and/or the external lines. Here we are interested in evaluating M' separately to leading order in a $1/Z$.

Without the logarithmic factor, Eq. (C1) can be evaluated analytically to be $4\pi\langle\delta(\mathbf{r}_{12})\rangle$. It can be shown that M' can be expanded as

$$\begin{aligned} M' &= 4\pi\langle\delta(\mathbf{r}_{12})\rangle[\ln(Z^2) + a_1 + a_2/Z + \cdots] \\ &= 4\pi\langle\delta(\mathbf{r}_{12})\rangle \ln(Z^2) + Z^3(A_1' + A_2'/Z + \cdots). \end{aligned} \tag{C2}$$

To compare with our calculation we are interested in the leading term in the $1/Z$ expansion. Neglecting higher-order terms in this expansion, we obtain the expression for M', which is given by Eq. (4.9), where $D = -(8/3)a_1 = -(16/3)A_1'$. A_1' can be determined by evaluating M' numerically to leading order in $1/Z$. There are contributions from the $1/Z$ perturbation of Ψ_0 originating from the ladder diagram in Fig. 1(a), as well as from the $1/Z$ perturbation V of the Hamiltonian operator originating from the crossed photon diagram in Fig. 1(b). The perturbation of E_0 of leading order in $1/Z$ does not contribute to M' due to the nondiagonal structure in the $\mathbf{p}$ operators. For M'', which is diagonal in the $\mathbf{p}$ operators, this last perturbation corresponds to

the reference-state part of the self-energy diagram with a Coulomb interaction on the outer line.

The expression for the $1/Z$ perturbation of Ψ_0 is straightforward to achieve and can be expanded in one-electron states. The evaluation of the perturbation in the Hamiltonian operator, however, needs more care. We evaluated the latter by using the expansion

$$\ln(H-E) = \ln(H_0-E_0) + \int_0^\infty dx \frac{1}{H_0-E_0+x}(V-E_1) \times \frac{1}{H_0-E_0+x} - \cdots \quad \text{(C3)}$$

for the logarithmic factor and get to leading order in $1/Z$ for the perturbation of the Hamiltonian operator

$$(H_0-E_0)\int_0^\infty dx \frac{1}{H_0-E_0+x}(V-E_1)\frac{1}{H_0-E_0+x} + (V-E_1)\ln(H_0-E_0), \quad \text{(C4)}$$

where x is a real integration variable. Before the x integration is performed we insert identity operators, expressed in one-electron states, around the perturbation. Only $|\,1snp\rangle$ and $|\,n'p1s\rangle$ states contribute for $\Psi_0 = |\,1s^2\rangle$ and we can replace $H_0 - E_0$ with $q = e_{np} - e_{1s}$ and $q' = e_{n'p} - e_{1s}$, respectively. The perturbation in Eq. (C4), for particular n and n', now becomes V times the integral (as mentioned E_1 does not contribute)

$$q'\int_0^\infty \frac{dx}{(q'+x)(q+x)} + \ln(q). \quad \text{(C5)}$$

Performing the x integration we obtain, for $q \neq q'$,

$$\frac{q}{q-q'}\ln(q) + \frac{q'}{q'-q}\ln(q'). \quad \text{(C6)}$$

For $q = q'$ the corresponding result is $1 + \ln(q)$.

We have evaluated all the $1/Z$ contributions to both M' and M'' and have reproduced the coefficient $A_1(1s^2\,{}^1S)$ calculated by Goldman and Drake [41] for the sum of the two. We obtain $-6.167\,40$ compared to their value $-6.167\,410(5)$. For the part corresponding to M' separately we obtain $A_1' = 0.357\,96$ leading to $D = -(16/3)A_1' = -1.9091$ to be used in Eq. (4.9). We have also achieved the same result from our two-photon exchange program by taking the Coulomb-Breit NVP retardation effect (retarded minus unretarded), making the dipole approximation and taking the limit when Z goes to zero. The low energy photon contribution is then taken by integrating the photon energy from zero to 1 a.u. and, which is important, neglecting the electron excitation energies q and q' in the upper limit. As already mentioned, this leads to unphysical results for the low photon energy contribution, but is consistent with the definition of M'.

[1] See, for instance, Proceedings of the Nobel Symposium 85, Heavy-Ion Spectroscopy and QED Effects in Atomic Systems, edited by I. Lindgren, I. Martinson, and R. Schuch [Phys. Scr. **T46**, 1 (1993)]; see also, I. Martinsson, At. Rep. Prog. Phys. **52**, 157 (1989); or A. E. Livingstone, J. Phys. (Paris) Colloq. **50**, C1-255 (1989).

[2] J. Sucher, Phys. Rev. A **22**, 348 (1990).

[3] E. Lindroth, J.-L. Heully, I. Lindgren, and A.-M. Mårtensson-Pendrill, J. Phys. B **20**, 1679 (1987); E. Lindroth, Phys. Rev. A **37**, 316 (1988).

[4] S. A. Blundell, W. R. Johnson, Z. W. Liu, and J. Sapirstein, Phys. Rev. A **39**, 3768 (1989).

[5] P. K. Kabir and E. E. Salpeter, Phys. Rev. **108**, 1256 (1957).

[6] J. Sucher, Phys. Rev. **109**, 1010 (1958); Ph.D. thesis, Columbia University, 1957.

[7] G. W. F. Drake, Adv. At. Mol. Phys. **18**, 399 (1988); Nucl. Instrum. Methods B **31**, 7 (1988).

[8] L. Labzowsky, V. Karasiev, I. Lindgren, H. Persson, and S. Salomonson, Phys. Scr. **T46**, 125 (1993).

[9] S. Blundell, P. J. Mohr, W. R. Johnson, and J. Sapirstein, Phys. Rev. A **48**, 2615 (1993).

[10] H. Persson, I. Lindgren, and S. Salomonson, Phys. Scr. **T46**, 125 (1993); I. Lindgren, H. Persson, S. Salomonson, and A. Ynnerman, Phys. Rev. A **47**, R4555 (1993).

[11] J. Schweppe *et al.*, Phys. Rev. Lett. **66**, 1434 (1991).

[12] S. Salomonson and P. Öster, Phys. Rev. A **40**, 5559 (1989); **40**, 5548 (1989).

[13] I. Lindgren, H. Persson, S. Salomonson, V. Karasiev, L. Labzowsky, A. Mitrushenkov, and M. Tokman, J. Phys. B **26**, L503 (1993).

[14] H. Persson, I. Lindgren, S. Salomonson, and P. Sunnergren, Phys. Rev. A **48**, 2772 (1993).

[15] A. Mitrushenkov, L. Labzowsky, I. Lindgren, H. Persson, and S. Salomonson (unpublished).

[16] I. Lindgren, Nucl. Instrum. Methods B **31**, 102 (1988).

[17] J. Sapirstein, Phys. Scr. **T46**, 52 (1993).

[18] I. Lindgren, Phys. Rev. A **31**, 1273 (1985).

[19] S. A. Blundell, W. R. Johnson, Z. W. Liu, and J. Sapirstein, Phys. Rev. A **40**, 2233 (1989).

[20] S. Salomonson and P. Öster, Phys. Rev. A **41**, 4670 (1990).

[21] S. Salomonson and A. Ynnerman, Phys. Rev. A **43**, 88 (1991).

[22] E. Lindroth, H. Persson, S. Salomonson, and A.-M. Mårtensson-Pendrill, Phys. Rev. A **45**, 1493 (1992).

[23] E. Lindroth and J. Hvarfner, Phys. Rev. A **45**, 2771 (1992).

[24] A.-M. Mårtensson-Pendrill, D. S. Gough, and P. Hannaford, Phys. Rev. A **49**, 3351 (1994).

[25] I. Lindgren, in *Relativistic, Quantum Electrodynamic, and Weak Interaction Effects in Atoms*, Proceedings of the Program held on Relativistic, Quantum Electrodynamic, and Weak Interaction Effects in Atoms at the Institute of Theoretical Physics, Santa Barbara, 1988, AIP Conf. Proc. No. 189, edited by Walter Johnson, Peter Mohr, and Joseph Sucher (AIP, New York, 1989), p. 371.

[26] M. H. Mittleman, Phys. Rev. A **4**, 893 (1971).

[27] P. Indelicato, O. Gorceix, and J. P. Desclaux, J. Phys. B **20**, 651 (1987); O. Gorceix and P. Indelicato, Phys. Rev. A **37**, 1087 (1988); O. Gorceix, P. Indelicato, and J. P. Desclaux, J. Phys. B **20**, 639 (1987); E. Lindroth

and A.-M. Mårtensson-Pendrill, Phys. Rev. A **39**, 3794 (1989).
[28] I. Lindgren, J. Phys. B **23**, 1085 (1990).
[29] J. Sucher, J. Phys. B **21**, L585 (1988).
[30] H. Araki, Prog. Theor. Phys. **17**, 619 (1957).
[31] V. M. Shabaev, Sov. Phys. J. **33**, 660 (1990).
[32] W. H. Furry, Phys. Rev. **81**, 115 (1951).
[33] M. H. Mittleman, Phys. Rev. A **5**, 2395 (1972); M. Gell-Mann and F. Low, Phys. Rev. **84**, 350 (1951).
[34] S. Love, Ann. Phys. (N.Y.) **113**, 153 (1978).
[35] W. R. Johnson and J. Sapirstein, Phys. Rev. Lett. **57**, 1126 (1986).
[36] W. R. Johnson, S. A. Blundell, and J. Sapirstein, Phys. Rev. A **37**, 307 (1988).
[37] W. R. Johnson and J. Sapirstein (private communication).
[38] A. M. Ermolaev, Phys. Rev. A **8**, 1651 (1975); Phys. Rev. Lett. **34**, 380 (1975).
[39] G. W. F. Drake, Adv. At. Mol. Phys. **18**, 399 (1982).
[40] W. R. Johnson and G. Soff, At. Data Nucl. Data Tables **33**, 405 (1985).
[41] G. W. F. Drake, in *Long-Range Casimir Forces: Theory and Recent Experiments on Atomic Systems,* edited by Frank S. Levin and David A. Micha (Plenum, New York, 1993), p. 164; S. P. Goldman and G. W. F. Drake, J. Phys. B **17**, L197 (1984).